A chemical and theoretical way to look at bonding on surfaces

Roald Hoffmann

Department of Chemistry and Materials Science Center, Cornell University, Ithaca, New York 14853-1301

An account is given of a theoretical approach to surface structure and reactivity that is within the framework of solid-state theory, yet strives for chemical ways of interpretation. One begins from highly delocalized band structures, but introduces interpretational tools (density-of-states decompositions, crystal orbital overlap populations) that allow a tracing of local, chemical acts. It is quite feasible to construct interaction diagrams for surfaces, and to make frontier orbital arguments, just as for molecules. There are some interesting ways in which the surface-adsorbate interaction differs from simple molecular binding—in particular, in the way that two-orbital four-electron and zero-electron interactions can turn into bonding. The surface and bulk acting as a reservoir of electrons or holes at the Fermi level are important in this context. Chemisorption emerges as a compromise in a continuum of bonding whose extremes are dissociative adsorption and surface reconstruction.

CONTENTS

I. INTRODUCTION AND OVERVIEW

A surface—be it of a metal, an ionic or covalent solid, or a semiconductor—is a form of matter with its own chemistry. In its structure and reactivity, it will bear resemblances to other forms of matter: bulk, discrete molecules in the gas phase and in solution, various aggregated states. And it will have differences. It is important to find the similarities and it is also important to note the differences—the similarities connect the chemistry of surfaces to the rest of chemistry; the differences are what make life interesting (and make surfaces economically useful).

Experimental surface science is a meeting ground of chemistry, physics, and engineering (Rhodin and Ertl, 1979; Somorjai, 1981). New spectroscopies have given us a wealth of information, be it sometimes fragmentary, on the ways that atoms and molecules interact with surfaces. The tools may come from physics, but the questions that are asked are very chemical—what is the structure and reactivity of surfaces by themselves, and of surfaces with molecules on them? In fact, a chemist who relaxes a little about the impressive surface probes will find an amusing phenomenological resemblance between current surface science studies and organic structure determinations by physical methods in the early days of the application of these methods, say the forties. Great stories, many of them true, are constructed about structures and reactions on the basis of a few evanescent bumps in an often hard-to-come-by spectrum.

The special economic role of metal and oxide *surfaces* in heterogeneous catalysis has provided a lot of the driving force behind current surface chemistry and physics. We always knew that it was at the surface that the chemistry took place. But it is only today that we are discovering the basic mechanistic steps in heterogeneous catalysis. It is an exciting time—how wonderful to learn precisely how Döbereiner's lamp and the Haber process work.

There have been an extraordinary number of theoretical contributions to surface science.[1] These have come from physicists and chemists, they have ranged from semiempirical molecular orbital (MO) calculations to state-of-the-art Hartree-Fock self-consistent-field+configuration interaction (CI) and advanced density func-

[1] I cannot provide here a bibliography of all theoretical studies in the surface area, because there are too many. Several reviews are available (Messmer, 1977; Gavezzotti and Simonetta, 1980; Cohen, 1984; Koutecký and Fantucci, 1986), but these do not do justice to the great volume of work in this area, especially that on the physical side. I do want to mention here the work of three groups that have made, in my opinion, important contributions to a chemical and theoretical understanding of surface reactions. One is that of Alfred B. Anderson, who has analyzed most important catalytic reactions, anticipating many of the results presented in this paper (Anderson, 1977; Anderson and Mehandru, 1984; Kang and Anderson, 1985, 1986; Mehandru and Anderson, 1986; Mehandru, Anderson, and Ross, 1986). Evgeny Shustorovich and Roger C. Baetzold, working separately and together, have both carried out detailed calculations and come up with an important perturbation-theory-based model for chemisorption phenomena (Shustorovich and Baetzold, 1983, 1985; Shustorovich, 1985, 1986, 1987; Baetzold, 1988). Christian Minot and co-workers have worked out some specific and general chemisorption problems (Minot *et al.*, 1983; Bigot and Minot, 1984; Garfunkel *et al.*, 1986; Minot, Bigot, and Hariti, 1986).

tional procedures. Some people have used atom and cluster models, some extended slab or film models for surfaces. Rather than providing a review of these methodologies and their results, I would like to present in this account some of the things my co-workers and I have learned about surface-molecule interactions from extended Hückel *band* calculations (Hoffmann and Lipscomb, 1962; Hoffmann, 1963).[2] This computational method is a very approximate one (all other methods are superior to it), but its transparency and the applicability to it of the simplest perturbation theoretic reasoning makes the method well suited to tracing origins and interactions. It should be mentioned at the outset that the methodology is not a self-consistent one, so electron drifts will be exaggerated. In addition, the calculations that will be reported here assume metal band orbitals doubly occupied by electrons, even for ferromagnetic surfaces. The rationalization that adsorbates reduce surface magnetism will not save the situation entirely, and occasionally such low-spin calculations will cause trouble. But the emphasis will be on the things the extended Hückel method gets right—bonding symmetry arguments, the fundamentals of a perturbation analysis.

The choice of a translationally extended system (i.e., two-dimensional film or slab model rather than a cluster) is intentional. The aim is to build a bridge to physics, to do the calculations in the framework or language with which most solid-state physicists are likely to feel comfortable. The special feature, which makes these calculations more than the lowest-quality band calculation, is that from the experience of chemistry and quantum chemistry we can construct the interpretational tools that will extract local, chemical actions from the delocalized orbitals. Whereas the calculations may be mediocre, on some absolute scale, the analysis is, I hope, perceptive and chemical.

In fact, I view the computations as just a stepping stone to what is really important. That is understanding, qualitative but powerful. With simple concepts of interaction, overlap, symmetry constraints, and bonding, we shall try to understand the structure and reactivity of molecules on surfaces. A central point of this work will be an extension to surfaces of a frontier orbital model, so useful in thinking about the reactions of discrete molecules.

II. SETTING UP: THE SURFACE AND THE ADSORBATE

The kind of problem that we want to study is how CO chemisorbs on Ni, how H_2 dissociates on a metal surface, how acetylene bonds to Pt(111) and then rearranges to vinylidene or ethylidyne, how surface carbide or sulfide affects the chemistry of CO, how CH_3 and CH_2 bind, migrate, and react on an iron surface. It makes sense to look first at structure and bonding in the stable or metastable configurations, the chemisorbed species. Then one can proceed to construct potential energy surfaces for motion of chemisorbed species on the surface, and eventually for reactions.

The very language I have used here conceals a trap. It puts the burden of motion and reactive power on the chemisorbed molecules, and not on the surface, which might be thought passive, untouched. Of course, this cannot be so. We now know that exposed surfaces reconstruct, i.e., make adjustments in structure driven by their unsaturation (Van Hove *et al.*, 1981; King, 1983; Inglesfield, 1985; Chan and Van Hove, 1986; Daum, Lehwald, and Ibach, 1986; Christmann, 1987; Kleinle *et al.*, 1987). They do so first by themselves, without any adsorbate. And they do it again, in a different way, in the presence of adsorbed molecules. The extent of reconstruction is great in semiconductors and extended molecules, small in molecular crystals and metals. The calculations I shall discuss deal with metal surfaces. One is then reasonably safe (we hope) if one assumes minimal reconstruction. It will turn out, however, that the signs of eventual reconstruction are to be seen even in these calculations.

It might be mentioned here that reconstruction is not a phenomenon reserved for surfaces. In the most important development in theoretical inorganic chemistry in the seventies, Wade (1971a, 1971b, 1972) and Mingos (1972) have provided us with a set of skeletal electron pair counting rules. These rationalize the related geometries of borane and transition-metal clusters. One aspect of their theory is that if the electron count increases or decreases from the appropriate one for the given polyhedral geometry, the cluster will adjust its geometry—open a bond here, close one there—to compensate for the different electron count. Discrete molecular transition-metal clusters and polyhedral boranes also reconstruct.

Returning to the surface, let us assume a specific surface plane cleaved out, frozen in geometry, from the bulk. That piece of the solid is periodic in two dimensions, semi-infinite, and aperiodic in the direction perpendicular to the surface. Half of infinity is much more painful to deal with than infinity, because translational symmetry is lost in that third dimension. And that symmetry is essential in simplifying the problem—one does not want to be diagonalizing matrices of the degree of Avogadro's number; with translational symmetry and the apparatus of the theory of group representations one can reduce the problem to the size of the number of orbitals in the unit cell.

So one chooses a slab of finite depth. Diagram 1 shows a four-layer slab model of a (111) surface of an fcc metal, a typical close-packed hexagonal face. How thick should the slab be? Thick enough so that its inner layers approach the electronic properties of the bulk, the outer layers those of the true surface. In practice, it is more often economics that dictates the typical choice of three

[2]The band-structure programs using the extended Hückel procedure evolved in my group in a collaborative effort involving many co-workers, who are listed in the Acknowledgments.

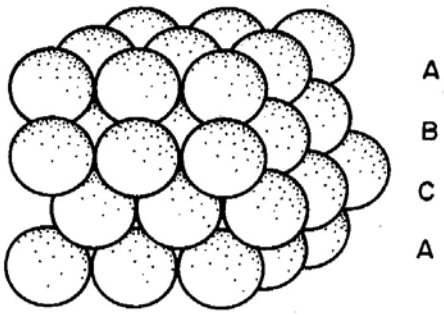

1

or four layers.

Molecules are then brought up to this slab. Not one molecule, for that would ruin the desirable two-dimensional symmetry, but an entire array or layer of molecules maintaining translational symmetry. This immediately introduces two of the basic questions of surface chemistry: coverage and site preference. Diagram 2 shows a $c(2\times2)$CO array on Ni(100), on-top adsorption,

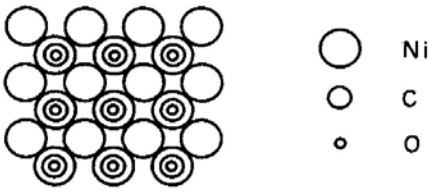

2

coverage $=\frac{1}{2}$. Diagram 3 shows four possible ways of adsorbing acetylene in a coverage of $\frac{1}{4}$ on top of Pt(111).

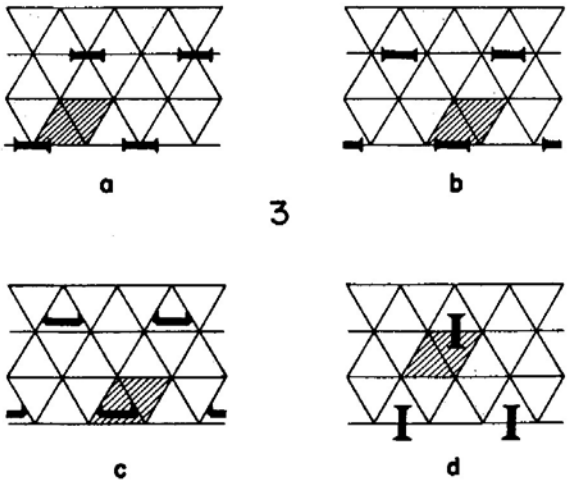

3

The hatched area is the unit cell. The experimentally preferred mode is the threefold bridging one, Diagram 3c. Many surface reactions are coverage dependent. And the position where a molecule sits on a surface, its orientation relative to the surface, is one of the things one wants to know.

III. HOW TO THINK ABOUT MANY ORBITALS

So we have a slab, three or four atoms thick, of a metal, and a monolayer of adsorbed molecules. The thicker the layer and the smaller the coverage, the more atoms in a unit cell. And there are many unit cells. If there are n valence orbitals in the unit cell (n might be ~ 100), and N microscopic unit cells in the macroscopic crystal (N approaches Avogadro's number), then there are Nn orbitals in all. That is a large number, hence the title of this section. At first sight, one is set back by the prospect of that myriad of levels. A person addicted to finding the causes of a geometrical or a stereochemical preference in the nature of *one* orbital (such as the author) might be particularly discouraged, for there is no way in the world that one orbital out of so many has the power to control or steer.

There is a way out of these quandaries. It is, first of all, symmetry—translational symmetry, leading to band structures and crystal orbitals—and, second, the language of densities of states. That language of solid-state theory[3] is, of course, part of the education of physicists. But chemists, in general, are unfamiliar with it. I need to introduce part of the formalism to the chemical audience, and I ask forbearance from my physicist readers as I go over things that are quite obvious to them (but that it might not hurt them to see again, without the crutch of the mathematical apparatus, which often serves as a substitute for real understanding). Those familiar with the band-structure and density-of-states formalism might skip ahead to Sec. V.

To introduce the idea of band structure, let us begin with a simple one-dimensional system, a chain of equally spaced H atoms (Diagram 4), or the isomorphic π system of a non-bond-alternating polyene (Diagram 5). Such

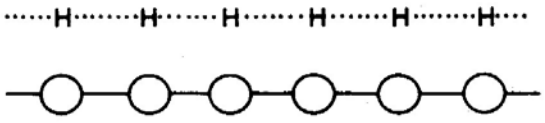

4

[3]In addition to the modern classic of Ashcroft and Mermin (1976), three other introductions to the field that are pedagogically effective and accessible to chemists might be cited, those of Altman (1970) and Harrison (1980a, 1980b). For a still more chemical perspective, very similar in spirit to the presentation here, see Burdett (1984), Albright, Burdett, and Whangbo (1985), Whangbo (1986), Hoffmann (1987), and Cox (1987).

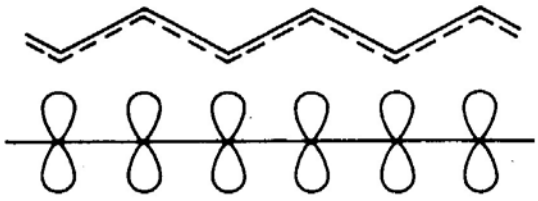

5

infinite chains can be modeled as an imperceptibly bent part of a very large ring. This is called applying cyclic boundary conditions.

The orbitals of the oligomers on the way to that very large ring are very well known (Diagram 6). In hydrogen (or ethylene) there is a bonding $\sigma_g(\pi)$ level below an antibonding $\sigma_u^*(\pi^*)$. In the three-membered ring (cyclic H_3, cyclopropenium) the pattern is 1 below 2; in cyclobutadiene we have 1 below 2 below 1,[4] and so on. Levels come in pairs, except for the lowest and, occasionally, the highest, and the number of nodes increases as one goes up in energy. We would expect the same for an infinite polymer, in the chemist's representation of a band of levels that is given at right in Diagram 6.

There is a neat way to write out all those orbitals in the band, making use of the translational symmetry. If we have a lattice whose points are labeled by an index $n = 0, 1, 2, 3, 4$, as shown in Diagram 7, and if on each lattice point there is a basis function (an H 1s orbital), χ_0, χ_1, χ_2, etc., then the appropriate symmetry-adapted

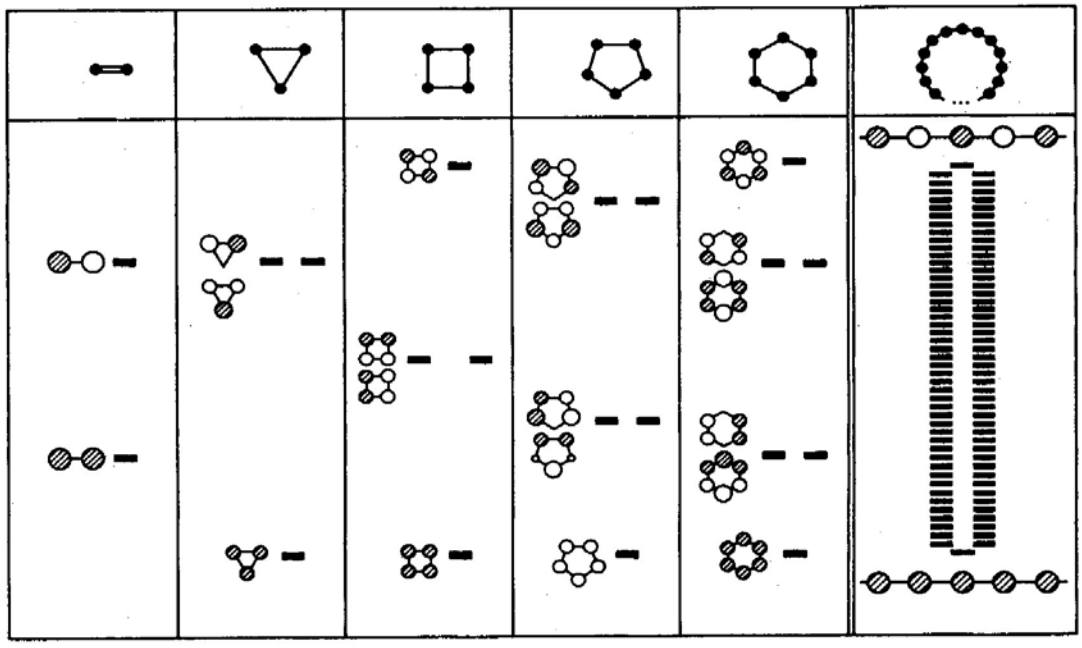

6

7

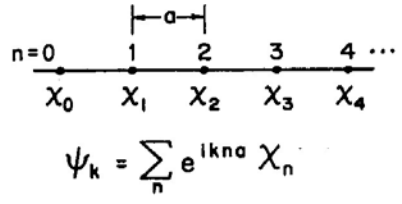

$$\psi_k = \sum_n e^{iknq}\chi_n$$

linear combinations are given in Diagram 7. Here a is the lattice spacing, the unit cell in one dimension, and k is an index that labels which irreducible representation of the translation group ψ transforms as. We shall see in a moment that k is much more, but for now k is just an index for an irreducible representation, just as a, e_1, e_2 in C_5 point group symmetry are labels.

The process of symmetry adaptation is called in the solid-state physics trade "forming Bloch functions" (footnote 3). To reassure a chemist that one is getting what one expects from Diagram 6, let us see in Diagram 8 what combinations are generated for two specific values of k, $k = 0$, and $k = \pi/a$. Referring back to Diagram 6, we see that the wave function corresponding to $k = 0$ is

[4]Throughout this paper I use a notation such that "lining" means a positive phase of the wave function, and the absence of lining means a negative phase. If you do not like that, the lining can be taken to mean negative ψ and no lining to mean positive ψ, thereby making the point that the absolute phase of ψ is immaterial.

8

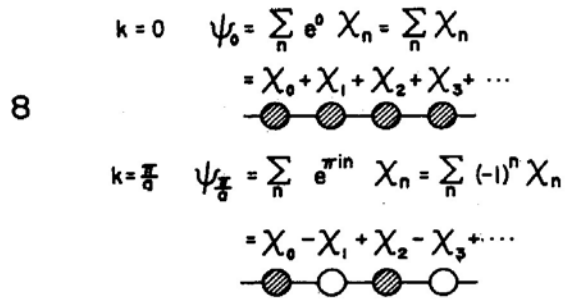

the most bonding one, the one for $k = \pi/a$ the top of the band. For other values of k we get a neat description of the other levels in the band. So k counts nodes as well. The larger the absolute value of k, the more nodes one has in the wave function. But one has to be careful—there is a range of k, and if one goes outside of it one does not get a new wave function, but repeats an old one. The unique values of k turn out to be in the interval $-\pi/a < k \leq \pi/a$ or $|k| \leq \pi/a$. This is called the Brillouin zone, the range of k.

How many values of k are there? As many as the number of translations in the crystal or, alternatively, as many as there are microscopic unit cells in the macroscopic crystal. So let us say Avogadro's number, give or take a few. There is an energy level for each value of k [actually two for each k, because there is an easily proved theorem that $E(k)=E(-k)$; most band structures do not draw the redundant $E(-k)$, but plot $E(|k|)$ and label it as $E(k)$]. The allowed values of k are equally spaced in the space of k, which is called reciprocal space. Remarkably k is not only a symmetry label and a node counter, but also a wave vector, and so related to momentum (footnote 3).

What a chemist then draws as a band in Diagram 6, repeated on the left in Diagram 9 (and the chemist tires

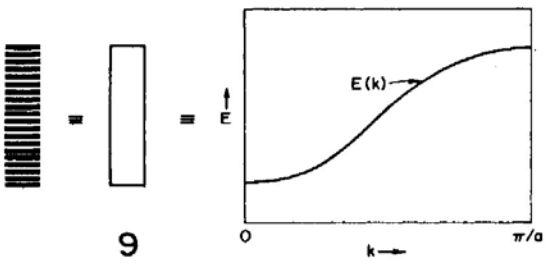

9

and draws ~20 lines or just a block instead of Avogadro's number), the physicist will alternatively draw as an $E(k)$ vs k diagram at right. Recall that k is quantized, and there is a finite, but large, number of levels in the diagram at right. The reason the curve looks continuous is that we have here a fine "dot matrix" printer at work—there are Avogadro's number of points in the diagram, giving the effect of a line.

Graphs of $E(k)$ vs k are called band structures. They can, of course, be much more complicated than this simple one. For instance, if we refer back to the CO on Ni(100) surface of Diagram 2, the band structure of the CO monolayer by itself is given in Fig. 1, and that of the underlying four-layer Ni slab by itself is in Fig. 2.[5]

At first sight, these figures appear to be too complicated to be understood, but this is not so.

(1) What is being plotted? E vs k. The lattice is two dimensional. k is now a vector, varying within a two-dimensional Brillouin zone, $k = k = (k_x, k_y)$. Some of the special points in this zone are given canonical names: Γ(the zone center) $= (0,0)$; $X = (\pi/a, 0)$; $M = (\pi/a, \pi/a)$. What is being plotted is the variation of the energy along certain specific directions in reciprocal space connecting these points.

(2) How many lines are there? As many as there are orbitals in the unit cell. In the case of CO, there is one molecule per unit cell, and that molecule has well-known 4σ, 1π, 5σ, $2\pi^*$ MO's. Each generates a band. In the case of the four-layer Ni slab, the unit cell has four Ni atoms. Each has five $3d$, one $4s$, and three $4p$ basis functions. We see some, but not all, of the many bands these orbitals generate in the energy window shown in Fig. 2.

(3) Where (in energy) are the bands? The bands spread out, more or less dispersed, around a "center of gravity." This is the energy of that orbital in the unit cell which gives rise to the band. Therefore, $3d$ bands lie below $4s$ and $4p$ for Ni, and 5σ below $2\pi^*$ for CO.

(4) Why are some bands steep, others flat? Because there is much inter-unit-cell overlap in one case, little in another. One very important feature of a band is its *dispersion*, or *bandwidth*, the difference in energy between the highest and lowest levels in the band. What determines the width of bands? The same thing that determines the splitting of levels in a dimer, ethylene, or H_2, namely, the overlap between neighboring unit cells. The greater the overlap between neighbors, the greater the bandwidth.

The CO monolayer bands in Fig. 1 are calculated at two different CO-CO spacings, corresponding to different coverages (Sung and Hoffmann, 1985). It is no surprise that the bands are more dispersed when the CO's are closer together. In the case of the Ni slab, the s,p bands are wider than the d bands, because the $3d$ orbitals are more contracted, less diffuse than the s,p.

(5) Why are the bands the way they are? They run

[5]The results shown here and elsewhere in this paper are taken from extended Hückel band calculations. These are essentially "tight-binding calculations," overlap included with the usual approximations of the extended Hückel method for the wave functions and Hamiltonian matrix elements. See footnote 2, Hoffmann and Lipscomb (1962); and Hoffmann (1963, 1987). For a specific discussion of the CO chemisorption calculations reported in this section, see Sung and Hoffmann (1985). There have been many other calculations for CO on metal surfaces, leading references to which may be found in Kasowski, Rhodin, and Tsai (1986).

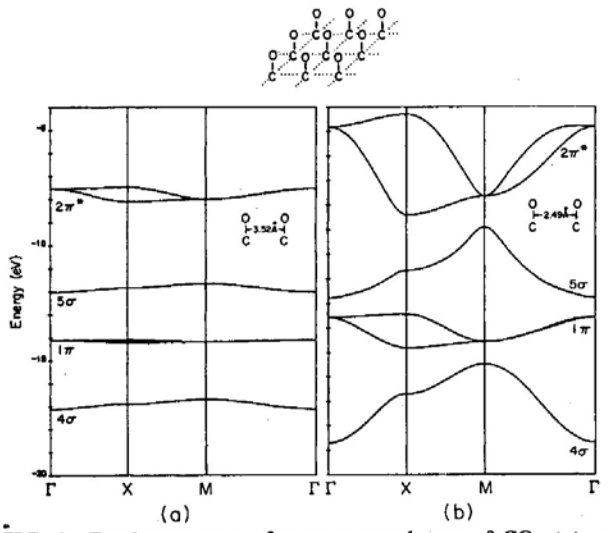

FIG. 1. Band structures of square monolayers of CO at two separations: (a) left, 3.52 Å; (b) right, 2.49 Å. These would correspond to half and full coverage, respectively, of a Ni(100) surface.

"up" and "down" (relative to Γ, say) along certain directions in the Brillouin zone as a consequence of symmetry and the topology of orbital interactions. Let me expand a little on this. Bands made out of s orbitals (or d_{z^2}) strung along a chain (as in Diagram 8 or 9) run "up"—the $k=0$ combination is at low energy. If the orbitals in question were p_z or $d_{xz,yz}$ (z is the propagation axis), the corresponding bands would run "down"—the $k=0$ combination would now be the most antibonding way to combine such orbitals (Hoffmann, 1987).

There are more details to be understood, to be sure. But, in general, these diagrams are complicated, not because of any mysterious phenomenon, but because of *richness,* the natural accumulation of understandable and understood components.

We still have the problem of how to talk about all these highly delocalized orbitals, how to retrieve a local, chemical, or frontier orbital language in the solid state. There is a way: perhaps we can talk about bunches of levels. There are many ways to group levels, but one fairly obvious one is to look at all the levels in a given energy interval. The density of states (DOS) is defined as follows:

$$\mathrm{DOS}(E)dE = \text{number of levels between } E \text{ and } E+dE\ .$$

For a simple band of a chain of hydrogen atoms, the DOS curve takes on the shape of Diagram 10. Note that

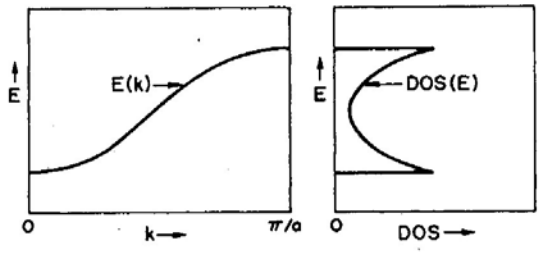

10

because the levels are equally spaced along the k axis, and because the $E(k)$ curve, the band structure, has a simple cosine curve, there are more states in a given energy interval at the top and bottom of this band. In general, DOS(E) is inversely proportional to the slope of $E(k)$ vs k or, to put it into plain English, the flatter the band, the greater the density of states at that energy. An illustration of this point is provided by the DOS of a hypothetical array of noninteracting adsorbates, for instance, an overlayer at very low coverage. The plot would show single lines (δ functions) at the energies of the MO's of one isolated adsorbate molecule.

The shapes of DOS curves are predictable from the band structures. Figure 3 shows the DOS curve for one of the CO monolayers. It could have been sketched from the band structure at left. In general, the construction of these is a job best left for computers.

The density-of-states curve counts levels. The integral of DOS up to the Fermi level is the total number of occupied MO's. Multiplied by two, it is the total number of electrons, so the DOS curves plot the distribution of electrons in energy.

One important aspect of the DOS curves is that they

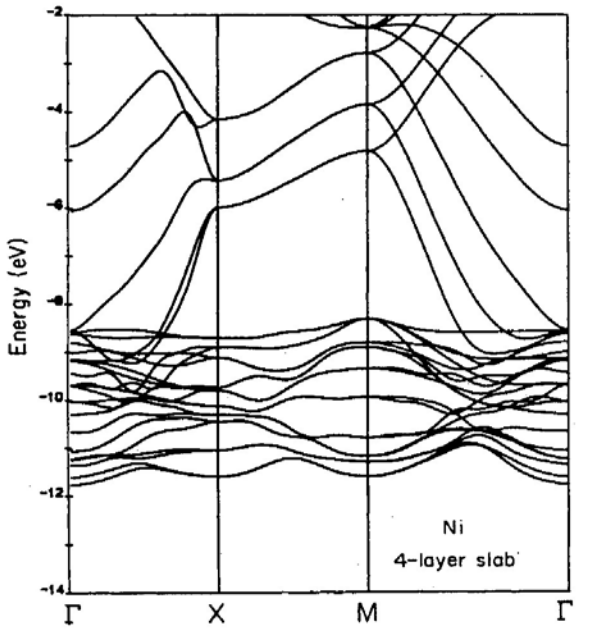

FIG. 2. The band structure of a four-layer Ni slab that serves as a model for a Ni(100) surface. The flat bands are derived from Ni 3d, the more highly dispersed ones above these are 4s,4p.

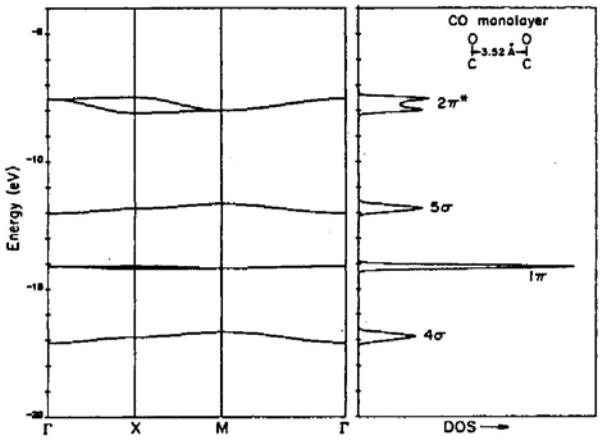

FIG. 3. The density of states (right) corresponding to the band structure (left) of a square monolayer of CO's, 3.52 Å apart.

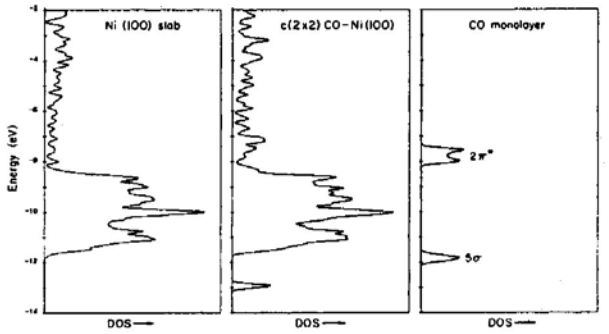

FIG. 4. The total density of states of a model $c(2\times2)$CO-Ni(100) system (center), compared to its isolated four-layer Ni slab (left) and CO monolayer components.

represent a return from reciprocal space, the space of k, to real space. The DOS is an average over the Brillouin zone, over all k that might give molecular orbitals of the specified energy. The advantage here is largely psychological. If I may be permitted to generalize, I think that chemists (with the exception of crystallographers), by and large, feel themselves uncomfortable in reciprocal space. They would rather return to, and think in, real space.

There is another aspect of the return to real space that is significant: *chemists can sketch the DOS of any material, approximately, intuitively.* All that is involved is a knowledge of the atoms, their approximate ionization potentials and electronegativities, and some judgment as to the extent of inter-unit-cell overlap (usually apparent from the structure). For an elaboration of this point, the reader is referred to another article discussing the general aspects of a theoretical and chemical approach to the solid state (Hoffmann, 1987).

To summarize: we go from orbitals in the unit cell (real space) to band structures (reciprocal space) to densities of states (back in real space). In the remainder of the paper, I shall be showing only densities of states, and we shall draw chemical arguments from these. Occasionally the crystal orbitals at certain k points will be required.

We still need two concepts—the solid-state analog of a charge distribution, and some bond index. But to introduce these, we shall use a specific surface problem.

IV. THE DETECTIVE WORK OF TRACING MOLECULE-SURFACE INTERACTIONS: DECOMPOSITION OF THE DENSITY OF STATES

We saw in the previous section the band structures and DOS of the CO overlayer and the Ni slab separately (Figs. 1–3) Now let us put them together in Fig. 4. The adsorption geometry is that shown in Diagram 2, with Ni-C 1.8 Å. Only the densities of states are shown, based on the band structures of Figs. 2 and 3. Some of the wriggles in the DOS curves are also not real; they are a result of insufficient k-point sampling in the computation.

It is clear that the composite system $c(2\times2)$CO-Ni(100) is roughly a superposition of the slab and CO layers. Yet things have happened. Some of them are clear—the 5σ peak in the DOS has moved down. Some are less clear—where is the $2\pi^*$, and which orbitals on the metal are active in the interaction?

These questions are basically ones of the location of electrons in space, a matter of abiding interest to chemists. Given a molecular orbital, we want to know how the electrons in that orbital are distributed. It is possible to do this for the highly delocalized Bloch functions as well, though not without a computer. Orbital by orbital, atom by atom, band by band, the computer partitions the electron density among the contributing orbitals or atoms. The procedure is called a Mulliken population analysis (Mulliken, 1955). It is repeated for several k points in the Brillouin zone, and then returns to real space by averaging over these points. These decompositions of the DOS are often called "projections of the DOS" or "local DOS" in the solid-state trade. The integral of these projections up to the Fermi level then gives the total electron density in a given atom or in a specified orbital.

Let us see how this decomposition helps to trace down the bonding in the chemisorbed CO system. Figure 5 shows the 5σ and $2\pi^*$ contributions to the DOS. The dotted line is a simple integration of the DOS of the fragment of contributing orbital. The relevant scale, 0–100 %, is to be read at the top. This integration shows the total percent of the given orbital that is occupied at a specified energy. It is clear that the 5σ orbital, though pushed down in energy, remains quite localized. Its occupation (the integral of this DOS contribution up to the Fermi level) is 1.62 electrons. The $2\pi^*$ orbital obviously is much more delocalized. It is mixing with the metal d band, and, as a result, there is a total of 0.74 electrons in the $2\pi^*$ levels together (Sung and Hoffmann, 1985).

Which levels on the metal surface are responsible for these interactions? We know that in discrete molecular systems the important contributions to bonding are for-

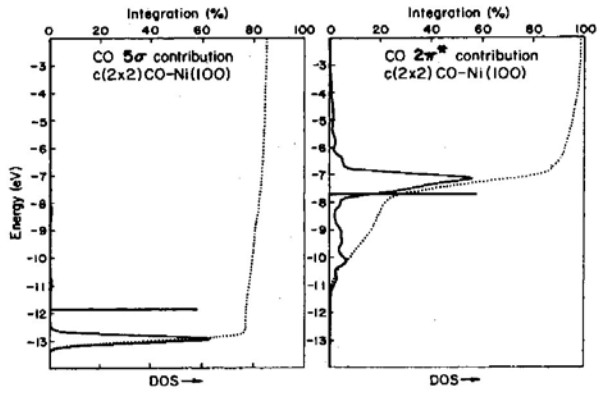

FIG. 5. The 5σ and $2\pi^*$ contributions to the total density of states for the $c(2\times2)$Co-Ni(100) model. Each contribution is magnified. The position of each level in isolated CO is marked by a line. The integration of the DOS contribution is given by the dotted line.

ward donation (Diagram 11a) from the carbonyl lone pair, 5σ, to some appropriate hybrid on a partner metal fragment, and back donation (Diagram 11b), involving

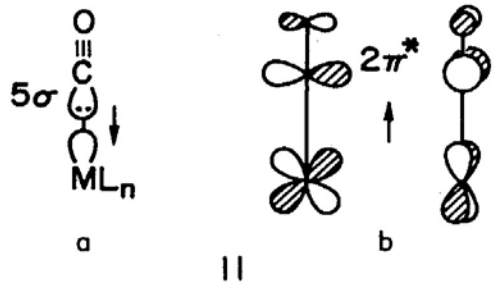

II

the $2\pi^*$ of CO and a d_π orbital, xz,yz, of the metal. We would suspect that similar interactions are operative on the surface.

These can be looked for by setting side by side the $d_\sigma(z^2)$ and 5σ contributions to the DOS, and $d_\pi(xz,yz)$ and $2\pi^*$ contributions. In Fig. 6 the π interaction is clearest: note how $2\pi^*$ picks up density where the d_π states are, and, conversely, the d_π states have a "resonance" in the $2\pi^*$ density. I have not shown the DOS of other metal levels, but were I to do so, it would be seen that such resonances are *not* found between those metal levels and 5σ and $2\pi^*$. The reader can confirm at least

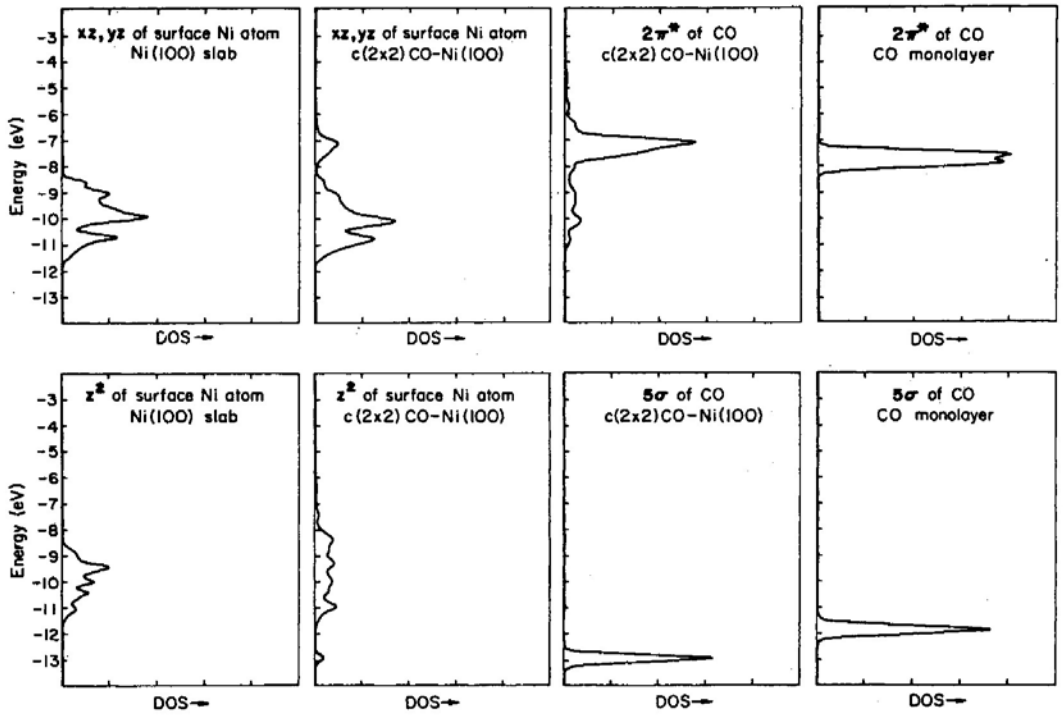

FIG. 6. "Interaction diagrams" for 5σ and $2\pi^*$ of $c(2\times2)$CO-Ni(100). The extreme left and right panels in each case show the contributions of the appropriate orbitals (z^2 for 5σ, xz,yz for $2\pi^*$) of a surface metal atom (left), and of the corresponding isolated CO monolayer MO. The middle two panels then show the contributions of the same fragment MO's to the DOS of the composite chemisorption system.

that 5σ does not pick up density in the vicinity of d_π states, nor $2\pi^*$ where d_σ states are mainly found. There is also some minor interaction of CO $2\pi^*$ with metal p_π states, a phenomenon not analyzed here.[6]

Let us consider another system in order to increase our familiarity with these fragment analyses. In Diagram 3 we drew several acetylene-Pt(111) structures with coverage $=\frac{1}{4}$. Consider one of these, the dibridged adsorption site alternative Diagram 3b redrawn in Diagram 12. The

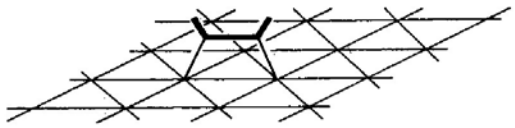

12

acetylene brings to the adsorption process a degenerate set of high-lying occupied π orbitals and an important unoccupied π^* set. These are shown at the top of Diagram 13. In all known molecular and surface complexes,

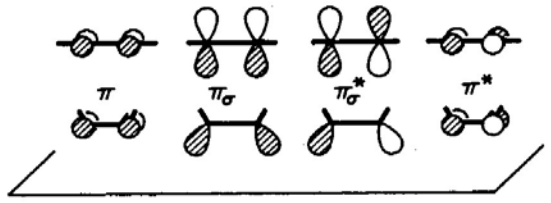

13

the acetylene is bent. This breaks the degeneracy of π and π^*, some s character mixing into the π_σ and π_{σ^*} components that lie in the bending plane and point to the surface. The valence orbitals are shown at the bottom of Diagram 13. In Fig. 7 we show the contributions of these valence orbitals to the total DOS of Diagrams 3b or 12. The sticks show the positions of the acetylene orbitals in the isolated molecule. It is clear that π and π^* interact less than π_σ and π_{σ^*}. And the overlap reasons behind that differential are obvious. Note the large effect on π_{σ^*}, analogous to what we saw for $2\pi^*$ of CO (Silvestre and Hoffmann, 1985).

A third system: in the early stages of dissociative H_2 chemisorption, one might imagine that H_2 approaches perpendicular to the surface, as in Diagram 14. Consider Ni(111), related to the Pt(111) surface we have discussed earlier. Figure 8 shows a series of three snapshots of the

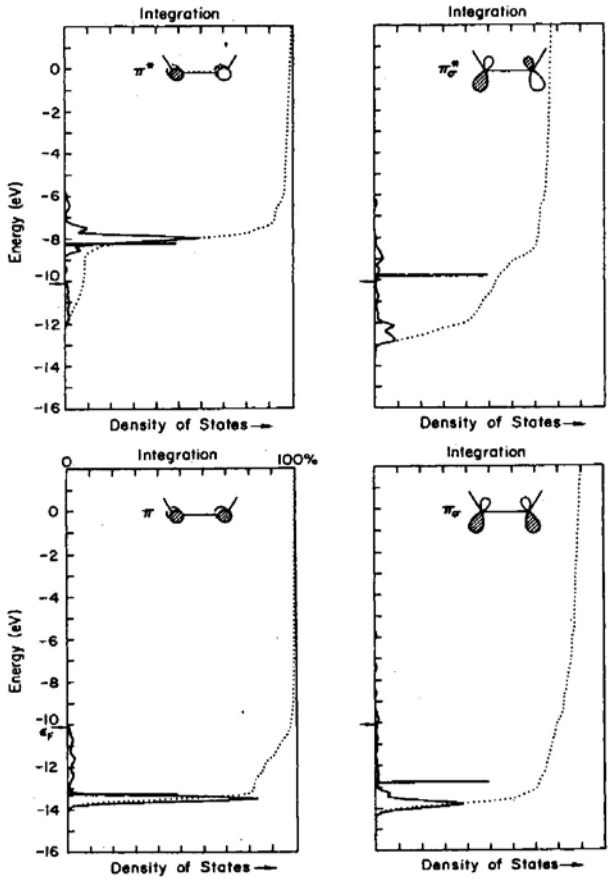

FIG. 7. Top: contributions of π^*, π^*_σ; bottom: π, π_σ to the density of states of C_2H_2 in a twofold geometry on Pt(111). The lines mark the positions of these levels in a free bent acetylene. The integrations of the DOS contributions are indicated by the dotted line.

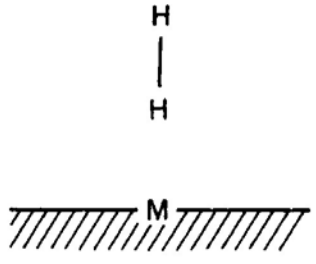

14

total DOS and its $\sigma_u^*(H_2)$ projection.[7] These are computed at separations of 3.0, 2.5, and 2.0 Å from the nearest

[6]The importance of this mixing has been stressed (Avouris, Bagus, and Nelin, 1986). We disagree on its magnitude, in that we find $p_{x,y}$ mixing into the main $2\pi^*$ density at -7 eV to be small. The COOP curve, to be shown later in Fig. 10, indicates that the density in this peak is Ni-C antibonding.

[7]These calculations are taken from Saillard and Hoffmann (1984). Other discussions of H_2 dissociative chemisorption have been published; see Siegbahn, Blomberg, and Bauschlicher (1984), Upton (1984), Harris and Anderson (1985), and references therein.

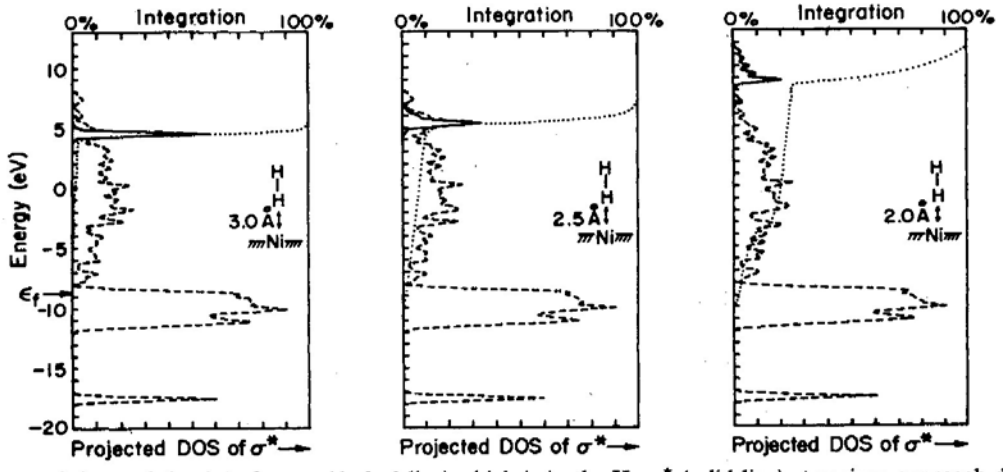

FIG. 8. That part of the total density of states (dashed line) which is in the H_2 σ_u^* (solid line) at various approach distances of a frozen H_2 to a Ni(111) surface model. The dotted line is an integration of the H_2 density.

H of H_2 to the Ni atom directly below it. The σ_g orbital of H_2 (the lowest peak in the DOS in Fig. 8) remains quite localized. But the σ_u^* interacts, is strongly delocalized, with its main density pushed up. The primary mixing is with the Ni s,p band. As the H_2 approaches, some σ_u^*, density comes below the Fermi level.

Why does σ_u^* interact more than σ_g? The classical perturbation theoretic measure of interaction

$$\Delta E = \frac{|H_{ij}|^2}{E_i^0 - E_j^0}$$

helps one to understand this. σ_u^* is more in resonance in energy, at least with the metal s,p band. In addition, its interaction with an appropriate symmetry metal orbital is greater than that of σ_g, at any given energy. This is the consequence of including overlap in the normalization:

$$\psi_\pm = \frac{1}{\sqrt{2(1\pm S_{12})}}(\phi_1 \pm \phi_2) .$$

The σ_u^* coefficients are substantially greater than those in σ_g. This has been pointed out by many people, but in the present context it has been emphasized by Shustorovich and Baetzold (1985; Shustorovich, 1985, 1986, 1987; Baetzold, 1988).[8]

[8]There is actually some disagreement in the literature on the relative role of C-H and H-H σ and σ^* levels in interactions with metal surfaces. A. B. Anderson (1977 and subsequent papers) finds σ donation playing the major role.

V. WHERE ARE THE BONDS?

When CO or acetylene chemisorb, partial bonds are formed to the surface. Bonds within the adsorbed molecule weaken, and we see the evidence for that directly in the diminished frequencies for specific vibrational modes, e.g., the CO stretch. It behooves us to look for a theoretical index of that bonding. This index, a COOP curve, which we shall define below, will allow us to push our detective investigation further and will help to restore a local, chemical viewpoint in an analysis of chemisorption.

The problem is how to find bonds in the highly delocalized bands. The idea is to extend the Mulliken population analysis to the crystal. Consider a two-center orbital:

$$\psi = c_1\phi_1 + c_2\phi_2 .$$

We want ψ to be normalized:

$$\int |\psi|^2 d\tau = 1 = \int |c_1\phi_1 + c_2\phi_2|^2 d\tau$$
$$= c_1^2 + c_2^2 + 2c_1c_2S_{12} .$$

Another way to think about the normalization is that it also gives the distribution of an electron in ψ. It is clear that the overlap term $2c_1c_2S_{12}$ is a characteristic of bonding. If the overlap integral S_{12} is taken as positive (and it can always be arranged so), then this quantity scales as we expect of a bond order: it is positive (bonding) if c_1 and c_2 are of the same sign, and negative if c_1 and c_2 are of opposite sign. The magnitude of this Mulliken "overlap population," for that is what $2c_1c_2S_{12}$ (summed over all orbitals on the two atoms, over all occupied MO's) is called, depends on c_i, c_j, S_{ij} (Mulliken, 1955).

Before we move into the solid, we might take a look at how these overlap populations might be used in a molec-

ular problem. Figure 9 shows the familiar energy levels of a diatomic, N_2, a "density-of-states" plot of these (just sticks proportional to the number of levels, of length one for σ, two for π), and the contributions of these levels to the overlap population. $1\sigma_g$ and $1\sigma_u$ (not shown in the figure) contribute little, because S_{ij} is small between tight 1s orbitals. $2\sigma_g$ is strongly bonding, $2\sigma_u$ and $3\sigma_g$ are essentially nonbonding. These are best characterized as lone pair combinations. π_u is bonding, π_g antibonding, $3\sigma_u$ the σ^* level. The right-hand side of Fig. 9 characterizes the bonding in N_2 at a glance. It tells us that maximal bonding will occur for seven electron pairs (counting $1\sigma_g$ and $1\sigma_u$), while more or fewer electrons will lower the N-N overlap population. It would be nice to have something like this for extended systems.

A bond indicator is easily constructed for the solid. An obvious procedure is to take all the states in a certain energy interval and examine their bonding proclivities, as measured by the Mulliken overlap population, $2c_ic_jS_{ij}$. What we are defining is an overlap population weighted density of states. The beginning of the obvious acronym (OPWDOS) unfortunately has been preempted by another common usage in solid-state physics. For that reason, we have called this quantity COOP, for crystal orbital overlap population.[9] It is also nice to think of the orbitals as working together to make bonds in the crystal, so the word is pronounced "co-op."

To get a feeling for this quantity, consider what a COOP curve for a hydrogen chain looks like. The simple band structure and DOS were given earlier, in Diagram 10; they are repeated with the COOP curve in Diagram 15.

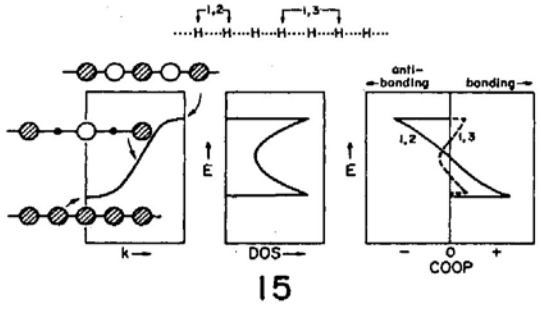

15

To calculate a COOP curve, one has to specify a bond. Let us take the nearest-neighbor 1,2 interaction. The bottom of the band is 1,2 bonding, the middle nonbonding, the top antibonding. The COOP curve obviously has the shape shown at the right in Diagram 15. But not all COOP curves look this way. If we specify the 1,3 next-nearest-neighbor bond (silly for a linear chain, not so silly

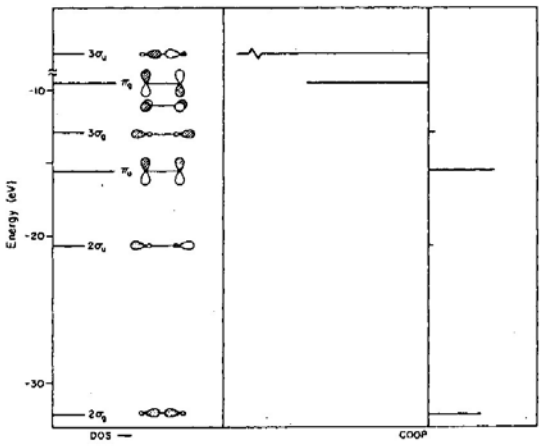

FIG. 9. The orbitals of N_2 (left) and a "solid-state way" to plot the density of states and crystal orbital overlap population curves for this molecule. The $1\sigma_g$ and $1\sigma_u$ orbitals are out of the range of this figure.

if the chain is kinked), then the bottom *and* the top of the band are 1,3 bonding, the middle antibonding. That curve, the dotted line in the drawing, is different in shape. And, of course, its bonding and antibonding amplitudes are much smaller because of the rapid decrease of S_{ij} with distance.

Note the general characteristics of COOP curves—positive regions that are bonding, negative regions that are antibonding. The amplitudes of these curves depend on the number of states in that energy interval, the magnitude of the coupling overlap, and the size of the coefficients in the MO's.

The integral of the COOP curve up to the Fermi level is the total overlap population of the specified bond. This points us to another way of thinking of the DOS and COOP curves. These are the differential versions of electronic occupation and bond order indices in the crystal. The integral of the DOS to the Fermi level gives the total number of electrons; the integral of the COOP curve gives the total overlap population, which is not identical to the bond order, but which scales like it. It is the closest a theoretician can get to the ill-defined but fantastically useful simple concept of a bond order.

Let us see how the COOP curve can be used to support the picture of CO chemisorption that was described above. The relevant curve is in Fig. 10. The solid line describes the Ni-C bonding, the dotted line C-O bonding. The C-O bonding is largely concentrated in orbitals that are out of the range (below) of this figure. Note the major contribution to Ni-C bonding in both the 5σ peak and the bottom of the d band. The 5σ contribution is due to σ bonding (Diagram 11a), but the bottom of the d band contributes through π bonding (Diagram 11b). This is evident from the "mirroring" C-O antibonding in the region. The antibonding component of that d_π-$2\pi^*$ interaction is responsible for the Ni-C and C-O antibonding above the Fermi level (Sung and Hoffmann, 1985).

[9]COOP was introduced for extended systems in papers by Hughbanks and Hoffmann (1983), Wijeyesekera and Hoffmann (1984), and Kertesz and Hoffmann (1984). An analogous index in the Hückel model, a bond order density, was introduced earlier by van Doorn and Koutecký (1977).

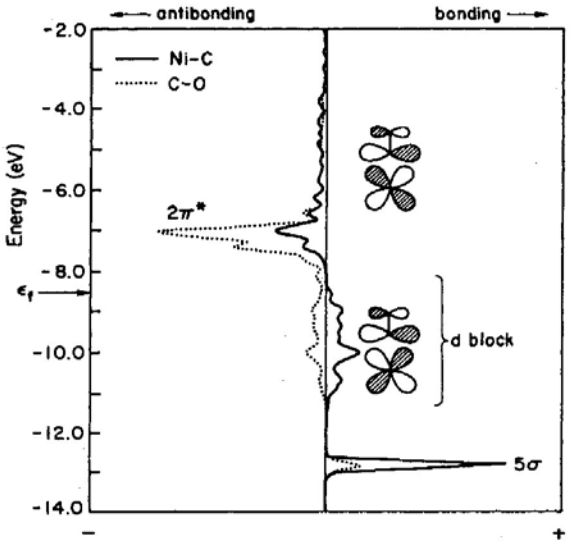

FIG. 10. Crystal orbital overlap population for CO, on top, in a $c(2\times2)$CO-Ni(100) model. Representative orbital combinations are drawn.

It may be useful to emphasize that these curves not only are descriptive, but also form a part of the story that allows us to trace down the interaction. For instance, supposing we were not so sure that it was the d_π-$2\pi^*$ interaction that was responsible for a good part of the bonding. Instead, we might have imagined π bonding between 1π and some unfilled d_π orbitals. The interaction is indicated schematically in Diagram 16. If this mixing

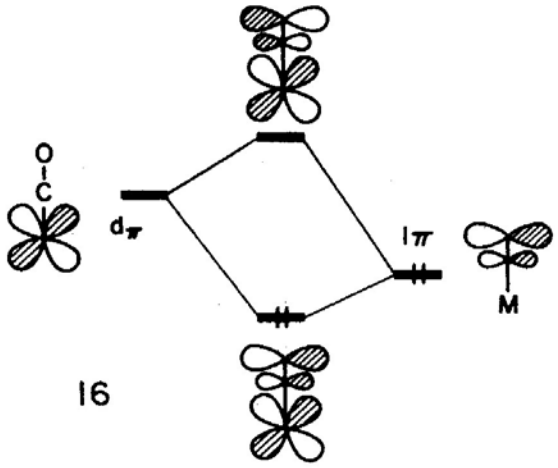

16

were important, the d-block orbitals, interacting in an antibonding way with 1π below them, should become in part Ni-C antibonding and C-O bonding. Nothing of this sort is seen in Fig. 9. The C-O antibonding in the d-block region indicates, instead, that $2\pi^*$ mixing is important.

Incidentally, the integrated overlap populations up to the Fermi level are Ni-C 0.84, C-O 1.04. In free CO the corresponding overlap population is 1.21. The bond weakening is largely due to population of $2\pi^*$ on chemisorption.

Another illustration of the utility of COOP curves is provided by the question of chemisorption site preference. On many surfaces, including Pt(111), a particularly stable dead end in the surface chemistry of acetylene is ethylidyne, CCH_3 (see footnote 5 in Silvestre and Hoffmann, 1985, and Kesmodel, Dubois, and Somorjai, 1979). How that extra hydrogen is picked up is a fascinating question. But let us bypass that and think about where the CCH_3 wants to be. Diagram 17a shows three alternatives—onefold or on-top, twofold or bridging, and threefold or capping. Experiment and theory show a great preference for the capping site. Why?

The important higher occupied and lower unoccupied orbitals of a carbyne, CR, are shown in Diagram 17b.

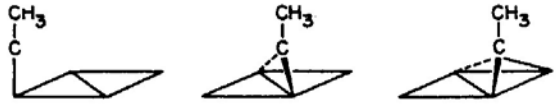

17a

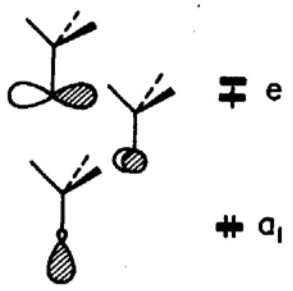

17b

The C $2p$ orbitals, the e set, are a particularly attractive acceptor set, certain to be important in any chemistry of this fragment. We could trace the involvement of this set in the three alternative geometries of Diagram 17a via DOS plots, but instead we choose to show in Fig. 11 the Pt-C COOP curve for onefold and threefold adsorption.

In both on-top and capping sites the carbyne e set finds metal orbitals to interact with. Bonding and antibonding combinations form. The coupling overlaps are much better in the capping site. The result is that the carbon-metal e-type antibonding combinations do not rise above the Fermi level in the onefold case, but do so in the threefold case. Figure 11 clearly shows this—the bonding and antibonding combinations are responsible for recognizable positive and negative COOP peaks. The total surface-CCH_3 overlap populations are 0.78 in the onefold case, 1.60 in the threefold case. The total energy follows these bonding considerations; the capping site is much preferred (Silvestre and Hoffmann, 1985).

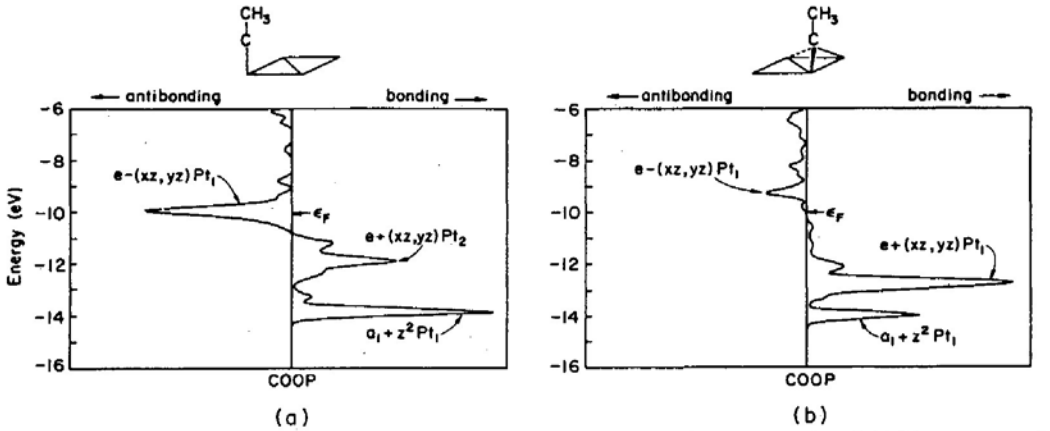

FIG. 11. Crystal orbital overlap population curve for the α-carbon-Pt_1 bond in onefold (a) and threefold (b) geometry of ethylidyne, CCH_3, on Pt(111).

VI. THE FRONTIER ORBITAL PERSPECTIVE

The analytical tools for moving *backward* from a band calculation to the underlying fundamental interactions are at hand. Now let us discuss the motion in the *forward* direction, the model of orbitals and their interaction, as analyzed by perturbation theory.

This is the frontier orbital picture.[10] A chemical interaction (between two parts of a molecule) or reaction (between two molecules) can be analyzed from the starting point of the energy levels of the interacting fragments or molecules. The theoretical tool one uses is perturbation theory. To second order, the interactions between two systems are pairwise additive over the MO's, and each pair interaction is governed by the expression

$$\Delta E = \frac{|H_{ij}|^2}{E_i^0 - E_j^0} .$$

That is what a wavy line in the interaction Diagram 18 indicates.

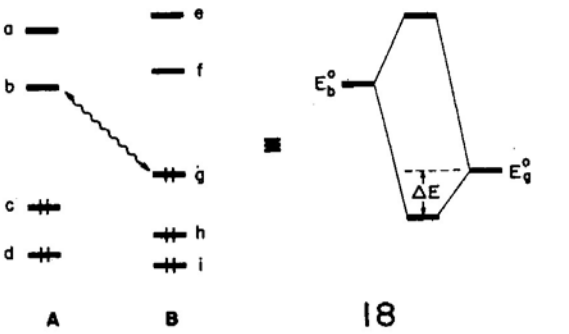

18

Individual interactions may be classified according to the total number of electrons in the two orbitals involved; thus ① and ② in Diagram 19 are two-electron interac-

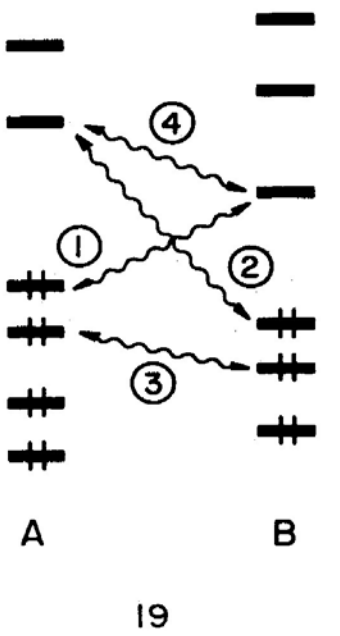

19

[10]The frontier orbital concept is a torrent into which flowed many streams. The ideas of Fukui were a crucial early contribution (Fukui, 1982, cites the relevant papers), as was the perturbation-theory-based PMO approach of Dewar (1969). The work of Salem was important (see Jorgensen and Salem, 1973, for references and a model portrayal, in the discussion preceding the drawings, of the way of thinking which my coworkers and I also espoused). The text of Albright, Burdett, and Whangbo (1985) carries through this philosophy for inorganic systems and is also an excellent source of references.

For surfaces, the frontier orbital approach is really there in the pioneering work of Blyholder (1964). In our work in the surface field, we first used this way of thinking in a side-by-side analysis of molecular and surface H-H and C-H activation (Saillard and Hoffmann, 1984). See also Grimley (1971, 1972); Thorpe (1972); Gadzuk (1974); van Santen (1984, 1986); and Albert and Yates (1987).

tions, ③ is four-electron, ④ is zero-electron. ① and ② are clearly stabilizing (see the right side of Diagram 18). This is where true bonding is found, with its range between covalent (orbitals balanced in energy and extent in space) and dative (orbitals that are unequal partners in the interaction, with charge transfer from donor to acceptor an inevitable correlate of bonding). Interaction ④ has no direct energetic consequences, since the bonding combination is unoccupied. And interaction ③ is repulsive, because what happens when the overlap is included in the calculations (Diagram 20) is that the antibonding

20

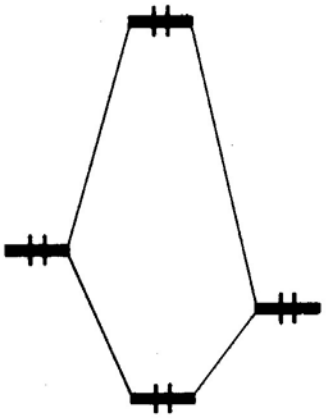

combination goes up more than the bonding one goes down. The total energy is greater than that of the separate isolated levels (Albright, Burdett, and Whangbo, 1985).

The electronic energy levels of molecules are separated by energies of the order of an electron volt. This makes them quantum systems *par excellence* and allows the singling out of certain levels as controlling a geometrical preference or a reactivity. For instance, in Diagram 18 acceptor level $|b\rangle$ of fragment A is closer in energy to donor level $|g\rangle$ of fragment B than are $|h\rangle$ and $|i\rangle$. If it should happen that the overlaps $\langle b|h\rangle$ and $\langle b|i\rangle$ are also much smaller than $\langle b|g\rangle$, then both the numerator and denominator of the perturbation expression would single out the $b(A)$-$g(B)$ interaction as an important, perhaps the most important, one. In general, it often turns out that the highest occupied molecular orbital (HOMO), or a small subset of higher-lying levels, and the lowest unoccupied molecular orbital (LUMO), or some subset of unoccupied MO's, dominates the interaction between two molecules. These are called the frontier orbitals. They are the valence orbitals of the molecule, the orbitals most easily perturbed in any molecular interaction. In them resides control of the chemistry of the molecule.

VII. ORBITAL INTERACTIONS IN THE SOLID

It is now clear that what the apparatus of densities of states and crystal orbital overlap populations has done is to restore to us a frontier orbital or interaction diagram way of thinking about the way molecules bond to surfaces. Whether it is $2\pi^*$ CO with d_π of Ni(100), or e of CR with some part of the Pt(111) band, in either case we can describe what happens in terms of local action. The only novel feature so far is that the interacting orbitals in the solid often are not single orbitals localized in energy or space, but bands.

A side-by-side comparison of orbital interactions in discrete molecules and of a molecule with a surface is revealing. Diagram 21a is a typical molecular interaction

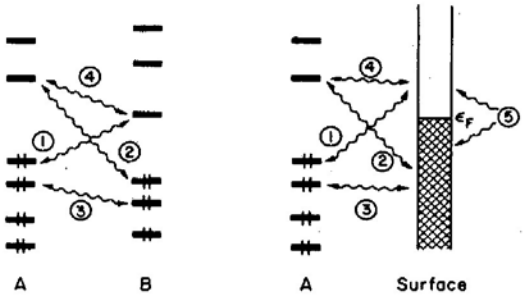

21

diagram, Diagram 21b a molecule-surface one. Even though a molecule is, in general, a many-level system, let us assume, in the spirit of a frontier orbital analysis, that a small set of frontier orbitals dominates. This is why the wavy lines symbolizing interaction go to the HOMO and LUMO of each component.

Within a one-electron picture the following statements can be made (and they apply to both the molecule and the surface unless specifically said not to do so).

(i) The controlling interactions are likely to be the two-orbital, two-electron stabilizing interactions ① and ②. Depending on the relative energy of the orbitals and the quality of the overlap, each of these interactions will involve charge transfer from one system to the other. In interaction ①, A is the donor or base, B, or the surface, the acceptor or acid. In interaction ②, these roles are reversed.

(ii) Interaction ③ is a two-orbital, four-electron one. It is destabilizing and repulsive, as Diagram 22a shows. In

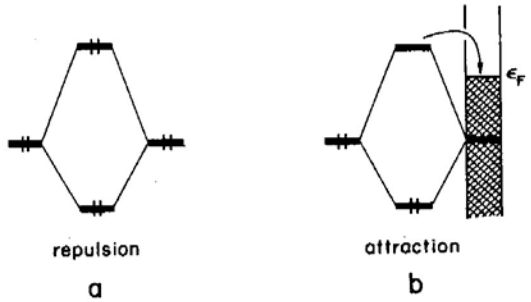

22

one-electron theories, this is where steric effects, lone pair repulsions, etc., are to be found (footnote 10). These interactions may be important. They may prevent bonding, that is, prevent interactions ① and ② from being realized. There is a special variant of this interaction which may occur in the solid, but is unlikely in discrete molecules. This is sketched in Diagram 22b—the antibonding component of a four-electron, two-orbital interaction may rise above the Fermi level. It will dump its electrons at the Fermi level and can no longer destabilize the system. Only the intersystem bonding combination remains filled.

The effect on molecule-surface bonding is clear—it is improved by this situation. What happens in the surface is less clear; let us defer discussion until we get to interaction ⑤.

(iii) Interaction ④ involves two empty orbitals. In general, it would be discounted as having no energetic consequences. This is strictly true in molecular cases (Diagram 23a). But in the solid, where there is a continuum

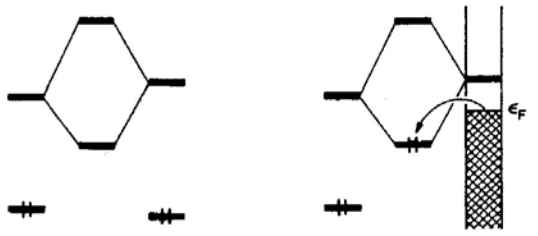

23

of levels, the result of such interaction may be that the bonding combination of the two interacting levels may fall below the Fermi level (Diagram 23b). Becoming occupied, it will enhance fragment A—surface bonding. Again, there may be an effect on the surface, because it has to supply the electrons for the occupation of that level.

(iv) Interaction ⑤ is unique to the metallic solid, something that follows from the states of the metal surface forming a near continuum. The interaction describes the second-order energetic and bonding consequences of shifts of electron density around the Fermi level. First-order interactions ①, ②, ③, and ④ all will move metal levels up and down. These metal levels, the ones that move, will belong to the atoms on the surface interacting with the adsorbate. The Fermi level remains constant—the bulk and surface are a nice reservoir of electrons. So electrons (holes) will flow in the surface and in the bulk underneath it, in order to compensate for the primary interactions. These compensating electrons or holes are not, however, innocent of bonding themselves. Depending on the electron filling, they may be bonding or antibonding in the bulk, between surface atoms not involved with the adsorbate, even in surface atoms so involved, but in orbitals that are not used in bonding to the chemisorbed molecule.

Before I leave this section, I should like to say quite explicitly that there is little novelty in the use my coworkers and I have made of interaction diagrams and perturbation theory applied to surfaces. A. B. Anderson has consistently couched his explanations in that language (Anderson, 1977; Anderson and Mehandru, 1984; Kang and Anderson, 1985, 1986; Mehandru and Anderson, 1986; Mehandru, Anderson, and Ross, 1986; see also subsequent references) and so have Shustorovich and Baetzold (1985; Shustorovich, 1985, 1986, 1987; Baetzold, 1988). Shustorovich's account of chemisorption is based on an explicit perturbation theoretic model (see also Varma and Wilson, 1980; Wilson and Varma, 1980; Andreoni and Varma, 1981). There is a very nice, quite chemical treatment of such a model in the work of Gadzuk (1974), based on earlier considerations (Grimley, 1971, 1972; Thorpe, 1972). van Santen (1984, 1986) draws interaction diagrams quite similar to ours. LaFemina and Lowe (1986) have recently discussed frontier crystal orbitals explicitly, and the interesting concept of interaction orbitals (Fujimoto, 1987a, 1987b) has recently been extended to surfaces (Fujimoto *et al.*, 1988). Salem and his co-workers (Salem and Leforestier, 1979; Salem and Elliott, 1983; Salem, 1985; Salem and Lefebvre, 1985) have developed a related perturbation theory based on a way of thinking about catalysis that includes a discussion of model finite Hückel crystals, privileged orbitals, generalized interaction diagrams, and the dissolution of adsorbate into catalyst bands. Several other papers have discussed interaction diagrams, privileged orbital sets or hybrids, or orbital symmetry considerations in the solid (Messmer and Bennett, 1972; Banholzer *et al.*, 1983, Masel, 1988).

Let us bring these interactions and interaction diagrams to life through some specific applications.

VIII. A CASE STUDY: CO ON Ni(100)

The Ni(100)-CO system already discussed seemed to provide an excellent example of the primary two-electron interactions at work. We found charge transfer from 5σ (its population going from 2.0 in the free CO to 1.62 in the CO-surface complex) and back donation from the surface to $2\pi^*$ (whose population rose from 0 to 0.74). Actually, there is an interesting wrinkle here, in that the four-electron and zero-electron interactions, mentioned in point (iii) above, manifest themselves.

To set a foundation for what we shall discuss, let us prepare a model molecular system for comparison. We shall build a metal-carbonyl bond between a model inorganic fragment, $d^6\ ML_5$, and a carbon monoxide. By $d^6\ ML_5$ we mean a transition-metal atom M, bonded to five ligands L ($L = H^-$, CO for instance) and containing six valence electrons. The interaction diagram Diagram 24, will be familiar to a chemist; the acceptor function of the ML_n fragment is provided by a low-lying *dsp* hybrid (Elian and Hoffmann, 1975). The two-electron bonding interactions are quite explicit. They result (M = Ni, $L = H^-$, M-H 1.7 Å, M-CO 1.9 Å) in a depopulation of

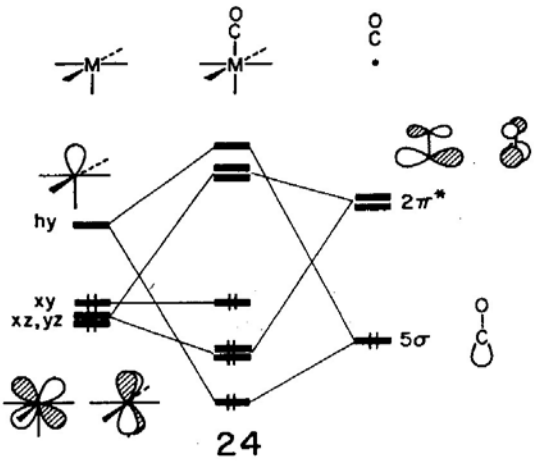

24

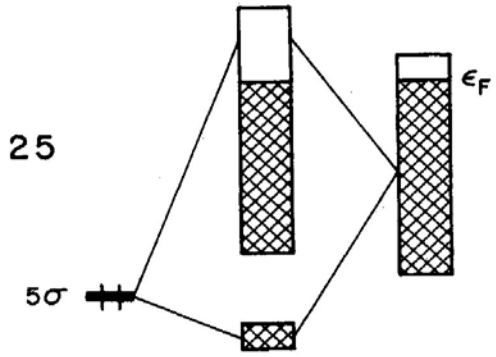

5σ by 0.41, and a population of $2\pi^*$ by 0.51 electrons. The metal functions involved in these interactions react correspondingly: so *xz,yz* loses 0.48 electrons, and the hybrid orbital gains 0.48. The net charge drifts are pretty well described by the sum of what happens in these orbitals: CO as a whole gain $0.01e^-$, and the ML_n fragment loses the same. The information is summarized in Table I.

If one just looks at the CO, what happens on the surface seems to be similar, as I noted above. And the d_π orbitals, *xz,yz*, are depopulated in $c(2\times2)$CO-Ni(100). But the d_σ, the z^2, the surface analog of the hybrid, actually *loses* electron density on chemisorption of CO.

What is happening here is that the CO 5σ is interacting with the entire z^2 band, but perhaps more with its bottom, where the coupling overlap is greater. The z^2 band is nearly filled ($1.93e^-$) in the metal slab. The net 5σ-d_σ band interaction would be repulsive, mainly due to four-electron two-orbital interactions, were it not for the pushing of some antibonding combinations above the Fermi level (see Diagram 25 for a schematic). The net result is some loss of z^2 density and comcomitant bonding. (The effect noted here has also been mentioned by Raatz and Salahub, 1984; Salahub and Raatz, 1984; Andzelm and Salahub, 1986.)

Where do those "lost" electrons go? Table I indicates that some, but certainly not all, go to the CO. Many are "dumped" at the Fermi level into orbitals that are mainly metal *d* band, but on the inner metal atoms, or on surface atoms not under CO. We shall return to the bonding consequences of these electrons, interaction ⑤, in a while.

Before leaving this instructive example, we note that the primary bonding interactions ① and ② are remarkably alike in the molecule and on the surface. These forward and back donations are, of course, the consequence of the classical Dewar-Chatt-Duncanson model of ethylene or another fragment bonding in an organometallic molecule (Dewar, 1951; Chatt and Duncanson, 1953). In the surface case, this is often termed the Blyholder model, the reference being to a perceptive early suggestion of such bonding for CO on surfaces (Blyholder, 1964). More generally, interactions ① and ② are the fundamental electronic origins of the cluster-surface analogy. This is a remarkably useful construction of a structural, spectroscopic, and thermodynamic link between organometallic chemistry and surface science (Muetterties, 1978, 1982; Muetterties and Rhodin, 1979). For an excellent comparison of structure bonding and reactivity in organometallic molecules and on surfaces, see Albert and Yates (1987).

IX. BARRIERS TO CHEMISORPTION

The repulsive two-orbital four-electron interaction that turns into an attractive, bonding force when the electrons, rising in energy, are dumped at the Fermi level is not just a curiosity. I think that it is responsible for observed kinetic barriers to chemisorption and the possible existence of several independent potential energy minima as a molecule approaches a surface.

Consider a model molecule, simplified here to a single occupied level, approaching a surface. Some schematic level diagrams and an associated total energy curve are drawn in Fig. 12. The approach coordinates translate

TABLE I. Some electron densities in a model H_3NiCo and the $c(2\times2)$CO-Ni(100) system.

	NiH_3^-	$NiH_3(CO)^-$	CO		Ni(100)	$c(2\times2)$CO-Ni(100)	CO
5σ	—	1.59	2.0	5σ	—	1.62	2.0
$2\pi^*$	—	0.51	0.0	$2\pi^*$	—	0.74	0.0
hy	0.0	0.48	—	d_σ[a]	1.93	1.43	—
d_π	4.0	3.52	—	d_π[a]	3.81	3.31	—
CO	—	10.01	10.0	CO	—	10.25	10.0
H_3Ni	16.0	15.99	—	Ni[a]	10.17[b]	9.37	—

[a]For those surface atoms which have CO on them.
[b]This number is not 10.0, because the surface layer of the slab is negative relative to the inner layer.

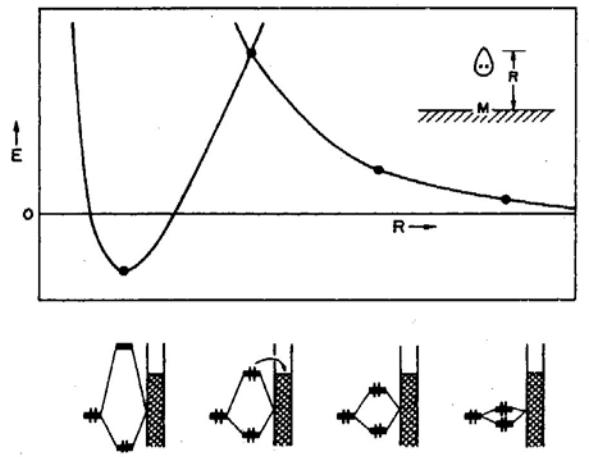

FIG. 12. A schematic drawing showing how the interactions of levels (bottom) can lead to a potential energy curve (top) which has a substantial barrier to chemisorption. R measures the approach of a molecule, symbolized by a single interacting electron pair, to a surface. At large R, repulsive four-electron interactions dominate. At some R (second point from left), the antibonding combination crosses the Fermi level and dumps its electrons. At shorter R there is bonding.

into electron interaction. Far away there is just repulsion, which grows as the molecule approaches the surface. But when the antibonding combination is pushed up to the Fermi level, the electrons leave it for the reservoir of hole states, empty metal band levels. Further interaction is attractive.

This simple picture was first given, to my knowledge, by Garfunkel and Minot and their co-workers (Garfunkel *et al.*, 1986; Garfunkel and Feng, 1986; Minot, Bigot, and Hariti, 1986; see also Raatz and Salahub, 1984; Salahub and Raatz, 1984; Shustorovich, 1985; Andzelm and Salahub, 1986). In reality, the repulsion at large metal adsorbate distances will be mitigated, and in some cases overcome, by attractive two-electron interactions of type ① or ②(see Diagram 21). But the presence of the interaction, I think, is quite general. It is responsible, in my opinion, for some of the large kinetic barriers to CO chemisorption and CH_4 decomposition measured in the elegant beam experiments of Ceyer, Madix, and their coworkers (Tang *et al.*, 1985, 1986; Steinruck, Hamza, and Madix, 1986; Hamza, Steinruck, and Madix, 1987; Lo and Ehrlich, 1987).

In reality, what we are describing is a surface crossing. And there may be not one, but several such, for it is not a single level, but groups of levels that are "pushed" above the Fermi level. There may be several metastable minima, precursor states, as a molecule approaches a surface.[11]

In this section we have mentioned, for the second time, the bonding consequences of emptying, at the Fermi level, molecular orbitals delocalized over adsorbate and surface, and antibonding between the two. Salahub (Salahub and Raatz, 1984; Raatz and Salahub, 1984; Andzelm and Salahub, 1986) and Anderson (Kang and Anderson, 1985, and papers cited therein) stress the same effect, as do in another context Harris and Anderson, (1985). There is a close relationship between this phenomenon and a clever suggestion made some time ago by Mango and Schachtschneider (1967; Mango, 1978) on the way in which metal atoms (with associated ligands) lower the activation barriers for forbidden concerted reactions. They pointed out that such electrons, instead of proceeding on to high antibonding levels, can be transferred to the metal. We, and others, have worked out the details of this kind of catalysis for some specific organometallic reactions, such as reductive elimination (Tatsumi *et al.*, 1981; Hoffmann, 1982). It is a quite general phenomenon, and we shall return to it again in Sec. XIII.

X. ANOTHER METHODOLOGY

As I mentioned earlier, there are many, many other theoretical calculations for surfaces. Most of them are just better ways of solving the wave equation for the complex system at hand, not necessarily leading to better chemical and physical understanding. There is one exception, the complex of ideas on chemisorption introduced and developed by Lundqvist, Nørskov, Lang, and their co-workers (Lang and Williams, 1976, 1978; Hjelmberg, Lundqvist, and Nørskov 1979; Nørskov and Lang, 1980; Lang, 1983; Lang and Nørskov, 1983; Lundqvist, 1983, 1984, 1986; Holloway, Lundqvist, and Nørskov, 1984). This is a methodology rich in physical understanding, and because of that and the fact that it provides a different way of looking at barriers for chemisorption, I want to mention the method explicitly here.

The methodology focuses, as many density functional schemes do, on the key role of the electron density. The Schrödinger equation is then solved self-consistently in the Kohn-Sham scheme (Kohn and Sham, 1965). Initial approaches dealt with a jellium-adatom system, which would at first sight seem rather unchemical, lacking microscopic detail. But there is much physics in such an effective medium theory, and with time the atomic details at the surface have come to be modeled with greater accuracy.

An example of the information the method yields is shown in Fig. 13, the total energy and density-of-states profile for H_2 dissociation on Mg(0001) (Lundqvist, Nørskov and Hjelmberg, 1981; Nørskov *et al.*, 1981; Nørskov, Holloway, and Lang, 1984). There are physisorption (P), molecular chemisorption (M), and dissociative chemisorption wells, with barriers in between. The primary controlling factor in molecular chemisorption is increasing occupation of H_2 σ_u^*, whose main density of states drops to the Fermi level and below as the H_2 nears the surface.

In this and other studies by this method one sees

[11]Several such minima have been compute in the interaction of atomic and molecular adsorbates with Ni clusters (Siegbahn, 1988).

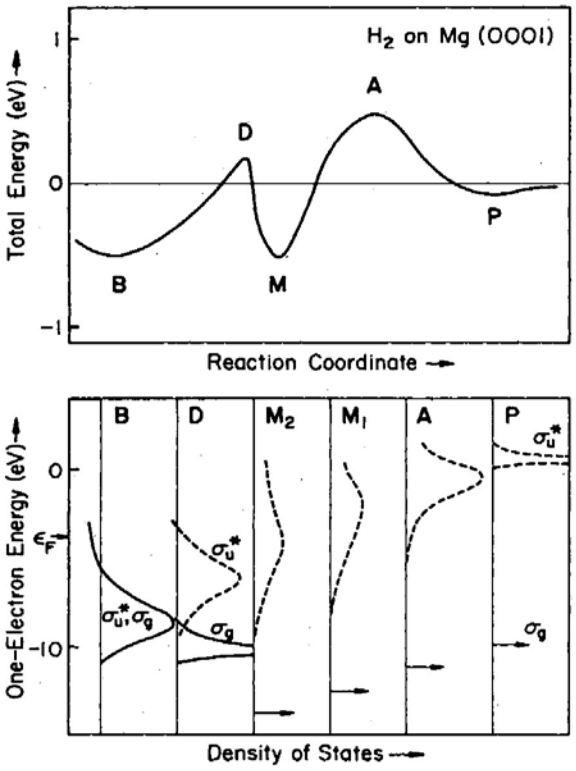

FIG. 13. Some calculated characteristics of H_2 on Mg(0001), after Nørskov *et al.* (1981; see also Lundqvist, Nørskov, and Hjelmberg, 1981, Nørskov, Holloway, and Lang, 1984). Top: schematic potential energy curve. P=physisorption minimum; M=chemisorbed molecule; B=chemisorbed atoms; A and D are transition states for chemisorption and dissociation. Bottom: development of the one-electron density of states at certain characteristic points. M_1 and M_2 correspond to two molecular chemisorption points, different distances from the surface. The dashed line is the σ_u^* density, moving to lower energy as the dissociation proceeds.

molecular levels, sometimes spread into bands, moving about in energy space. But the motions seem to be different from those calculated by the extended Hückel procedure. Figure 8 showed for H_2 on Ni some σ_u^* density coming below the Fermi level.[12] The main peak of σ_u^* however, was pushed up, as a simple interaction diagram might suggest, and in apparent disagreement with the result of Fig. 13. Perhaps (I am not sure) one way to reconcile the two pictures is by recognizing that mine is not self-consistent and does not account for proper screening of H_2 as it approaches the surface. It is possible that, if self-consistency or screening by electrons in the metal were included in the one-electron formalism, the pictures could be reconciled. There is also less discrepancy between the two approaches than one might imagine. In the reaction coordinate of Fig. 13 the H—H bond is stretched along the progression $P \rightarrow A \rightarrow M_1 \rightarrow M_2 \rightarrow D \rightarrow B$. σ_u^* drops precipitously, in our calculations as well, as the H—H bond is stretched.

The barriers to chemisorption in the work of Nørskov *et al.* come from the initial dominance of "kinetic energy repulsion." This is the Pauli effect at work, and I would like to draw attention to the correspondence between our four-electron repulsion and this kinetic energy effect. The problem (as usual) is that different models are built in different parts of physical reality. It becomes very difficult to compare them. The reason the effort is worth making is that the Lundqvist-Nørskov-Lang model has proven itself remarkably useful in revealing trends in chemisorption. It is physically and chemically appealing.

XI. CHEMISORPTION IS A COMPROMISE

Consider again the basic molecule-surface interaction, Diagram 26, now drawn specifying the bonding within

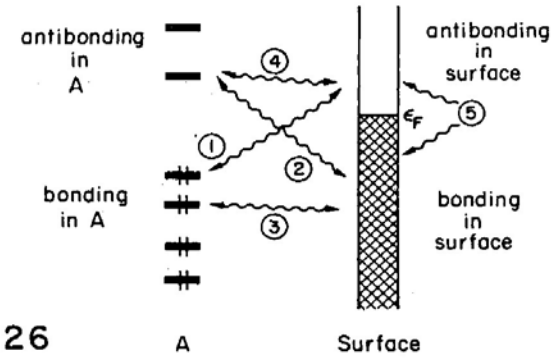

each component. The occupied orbitals of the molecule A are generally bonding or nonbonding within that molecule, the unfilled orbitals of A are usually antibonding. The situation on the metal depends on where in a band the Fermi level lies: the bottom of the d band is metal-metal bonding, the top is metal-metal antibonding. This is why the cohesive energy of the transition metals reaches a maximum around the middle of the transition series. Most of the metals of catalytic interest are in the middle or right part of the transition series. It follows that at the Fermi level the orbitals are generally metal-metal antibonding.

What is the effect of the various interactions on bonding within and between the adsorbate and the surface? Interaction ① and ② are easiest to analyze—they bind the molecule to the surface, and in the process they transfer electron density from generally bonding orbitals in one component to antibonding orbitals on the other. The net result: a bond is formed between the adsorbed molecule A and the surface. But bonding within the surface and within A is weakened.

Schematically this is indicated in Diagram 27. What about interactions ③ and ④? For moderate interaction ③ is repulsive and ④ has no effect. Neither does any-

[12]Figure 8 is for a perpendicular H_2 approach. We should really compare a parallel one to the Mg case, and the features of that parallel approach, while not given here, resemble Fig. 8.

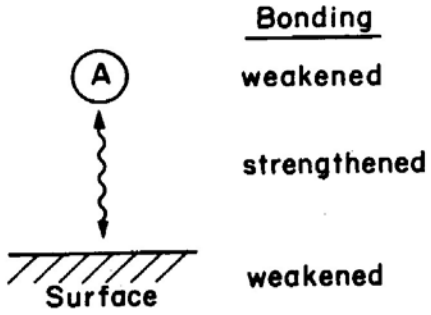

27

thing to bonding within A or the surface. When interaction grows, and antibonding (③) or bonding (④) states are swept past the Fermi level, these interactions provide molecule-surface bonding. At the same time, they weaken bonding in A, transferring electron density into antibonding levels and out of bonding ones. The effect of such strong interaction, or type ③ or ④ or, more generally, of second-order electron shifts, type ⑤, on bonding within the surface depends on the position of the Fermi level and the net electron drift.

The sum total of these interactions is still the picture of Diagram 27: *metal-adsorbate bonding is accomplished at the expense of bonding within the metal and the adsorbed molecule.* This is the compromise alluded to in the heading of this section.

A specific case will illustrate this compromise and point to an important consequence of this very simple notion.

Earlier we drew four possible geometries (Diagram 3) for a layer of acetylene, coverage $=\frac{1}{4}$, on top of Pt(111). Table II shows some of the indices of the interaction in the four alternative geometries, in particular the occupations of the four acetylene fragment orbitals ($\pi, \pi_\sigma, \pi^*_\sigma, \pi^*$), the various overlap populations, and calculated binding energies.

The threefold bridging geometry (Diagram 3c) is favored, in agreement with experiment and other theoretical results (Silvestre and Hoffmann, 1985). One should say right away that this may be an accident—the extended Hückel method is not especially good at predicting binding energies. The twofold (Diagram 3b) and fourfold (Diagram 3d) sites are slightly less bound, but more stable than the onefold site (Diagram 3a). But this order of stability is *not* a reflection of the extent of interaction. Let us see how and why this is so.

The magnitude of interaction could be gauged by looking at the acetylene fragment orbital populations or the overlap population. In the detailed discussion of the twofold site in an earlier section, we saw π and π^* more or less unaffected, and π^*_σ occupied. As a consequence, Pt—C bonds are formed, the C—C bond is weakened, and (interaction ⑤) some Pt—Pt bonds on the surface are weakened. A glance at the fragment MO populations and overlap populations in Table II shows that all this happens much more in the fourfold site in Diagram 3d—note that even π and π^* get strongly involved. The most effective interaction here is that shown in Diagram 28. Note that it is primarily of type ④.

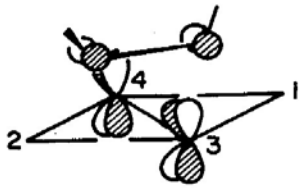

28

TABLE II. Bonding characteristics of several acetylene adsorption sites on Pt(111).

	C_2H_2	Bare surface				
Binding energy[a] (eV)			3.56	4.68	4.74	4.46
Overlap population						
C-C	1.70		1.41	1.32	1.21	1.08
Pt_1-Pt_2		0.14	0.12	0.08	0.09	−0.02
Pt_2-Pt_3		0.14	0.14	0.13	0.07	0.06
Pt_1-Pt_4		0.14	0.13	0.13	0.15	0.06
Pt_1-C[b]			0.30	0.54	0.52	0.33
Pt_3-C			0.00	0.01	0.19	0.27
Occupations						
π^*	0.0		0.08	0.17	0.33	0.53
π^*_σ	0.0		0.81	1.06	1.03	0.89
π_σ	2.0		1.73	1.59	1.59	1.57
π	2.0		1.96	1.96	1.73	1.53

[a]Taken as the difference: E(slab) + $E(C_2H_2)$-E(geometry) in eV.
[b]The carbon atom here is the closest to the particular Pt atom under consideration.

By any measure, interaction is least in the on-top or onefold geometry, most in the fourfold one. See, for instance, the trend in C-C overlap populations, or the Pt—Pt bond weakening. In the fourfold geometry, the Pt-Pt overlap population is even negative—bonding between metal atoms in the surface is being destroyed. It is clear that the favorable condition for chemisorption, or the preference of a hydrocarbon fragment for a specific surface site, is determined by a balance between increased surface-adsorbate bonding and loss of bonding within the surface or in the adsorbed molecule.

Adsorbate-induced surface reconstruction and dissociative chemisorption are merely natural extremes of this delicate balance. In each case, strong surface-adsorbate interactions direct the course of the transformation, either breaking up bonding in the surface, so that it reconstructs, or disrupting the adsorbed molecules. An incisive discussion of the latter situation, for the case of acetylene on iron and vanadium surfaces, has been provided by A. B. Anderson (Anderson and Mehandru, 1984; Kang and Anderson, 1986).

XII. QUALITATIVE REASONING ABOUT ORBITAL INTERACTIONS ON SURFACES

The previous sections have shown that one can work back from band structures and densities of states to local chemical actions—electron transfer and bond formation. It may still seem that the qualitative construction of surface-adsorbate orbital interaction diagrams, in the forward direction, is difficult. There are all these orbitals. How does one estimate their relative interaction?

Symmetry and perturbation theory make such a forward construction relatively simple, as they do for molecules. First, in extended systems the wave vector k is also a symmetry label, classifying different irreducible representations of the translation group. In molecules, only levels belonging to the same irreducible representation interact. Similarly, in the solid only levels of the same k can mix with each other.

Second, the strength of any interaction is measured by the same expression as for molecules:

$$\Delta E = \frac{|H_{ij}|^2}{E_i^0 - E_j^0} .$$

Overlap and separation in energy are important and can be estimated.

There are some complicating consequences of there being a multitude of levels, to be sure. Instead of just saying "this level does (or does not) interact with another one," we may have to say "this level interacts more (or less) effectively with such and such part of a band." Let me illustrate this with some examples.

Consider the interaction of methyl, CH_3, with a surface, in on-top and bridging sites, Diagram 29 (Zheng,

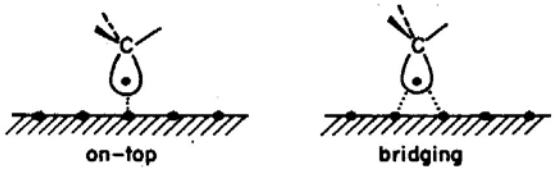

29

Apeloig, and Hoffmann, 1988), Let us assume low coverage. The important methyl orbital is obviously its nonbonding or radical orbital n, a hybrid pointing away from the CH_3 group. It will have the greatest overlap with any surface orbitals. The position of the n orbital in energy is probably just below the bottom of the metal d band. How do we analyze the interactions of metal and methyl?

It is useful to take things apart and consider the metal levels one by one. Diagram 30 illustrates schematically

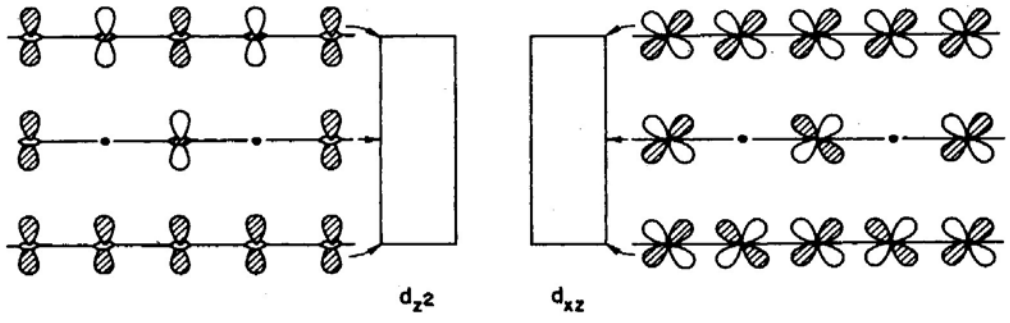

30

some representative orbitals in the z^2 and xz bands. The orbitals at the bottom of a band are metal-metal bonding, those in the middle nonbonding, and those at the top of the band antibonding. While things are assuredly more complicated in three dimensions, these one-dimensional pictures are indicative of what transpires.

The methyl radical orbital (it is really a band, but the band is narrow for low coverage) interacts with the entire

z^2 and xz bands of the metal, except at a few special symmetry-determined points where the overlap is zero. But it is easy to rank the magnitude of the overlaps, as I have done in Diagram 31 for on-top adsorption.

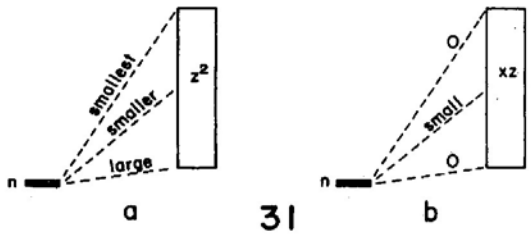

31

n interacts with the entire z^2 band, but because of the better energy match, more strongly so with the bottom of the band, as Diagram 32 shows. For interaction with xz, the overlap is zero at the top and bottom of the band, and never very efficient elsewhere (Diagram 33). For adsorption in the bridge, as in Diagram 28b, we would estimate the overlaps to go as Diagram 34. There is nothing mysterious in these constructions. The use of the perturbation theoretic apparatus, and specifically the role of k in delimiting interactions on surfaces, goes back to the work of Grimley (1971, 1972) and Gadzuk (1974), and has been consistently stressed by Salem (1985).

For a second example, we return to acetylene on Pt(111), specifically, in the twofold and fourfold geometries (Silvestre and Hoffmann, 1985). In the twofold geometry, we saw earlier (from the decomposition of the DOS) that the most important acetylene orbitals were π_σ and π_σ^*. These point toward the surface. Not surprisingly, their major interaction is with the surface z^2 band. But π_σ and π_σ^* interact preferentially with different parts of the band, picking out those metal surface orbitals which have similar nodal patterns to that of the adsorbate. Diagram 35 shows this—in the twofold geometry at hand the π_σ orbital interacts better with the bottom of the surface z^2 band and the π_σ^* with the top of that band.

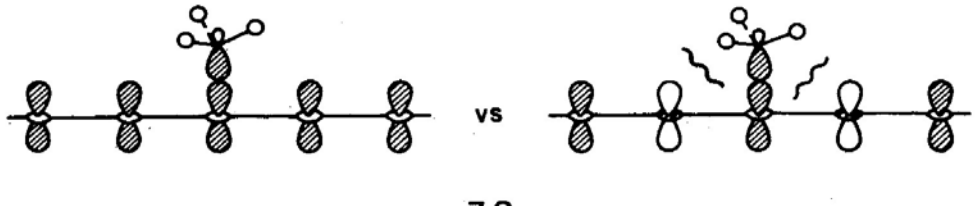

32

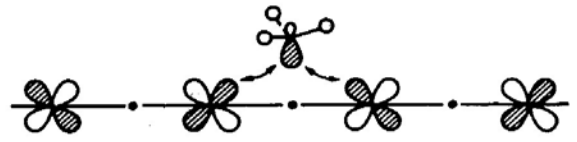

33

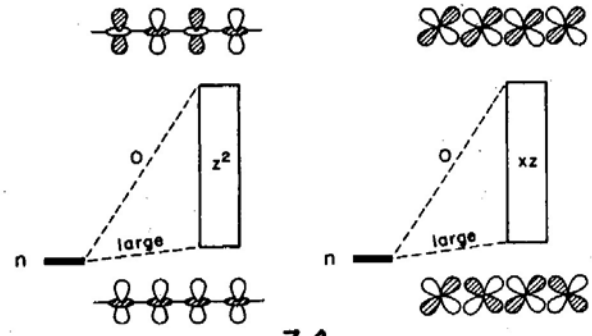

34

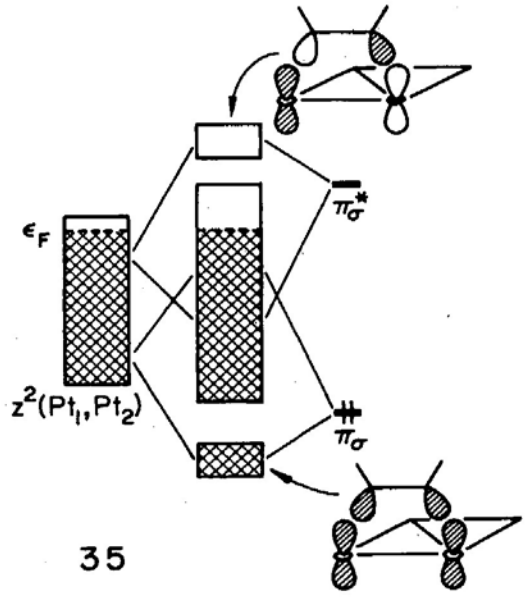

35

Note the "restructuring" of the z^2 band that results: in that band some metal-metal bonding levels that were at the bottom of the band are pushed up, while some of the metal-metal antibonding levels are pushed down. Here, very clearly, is part of the reason for weakening of metal-metal bonding on chemisorption.

I pointed out earlier that fourfold site chemisorption

was particularly effective in weakening the surface bonding, and transferring electrons into π^* as well as π_σ^*, thus also weakening C—C bonding. The interaction responsible was shown in Diagram 27. Note that it involves the overlap of π^* specifically with the top of the xz band. Two formally empty orbitals interact strongly, and their bonding component (which is antibonding within the metal and within the molecule) is occupied.

In general, it is possible to carry over frontier orbital arguments, the language of one-electron perturbation theory, to the analysis of surfaces.

XIII. THE ROLE OF THE FERMI LEVEL

Ultimately one wants to understand the catalytic reactivity of metal surfaces. What we have learned experimentally is that reactivity depends in interesting ways on the metal, on the surface exposed, on the impurities or coadsorbates on that surface, on defects, on the coverage of the surface. Theory is quite far behind in understanding these determining factors of surface reactivity, but some pieces of understanding emerge. One such is the role of the Fermi level.

The Fermi level in all transition series falls in the d band—if there is a total of x electrons in the $(n)d$ and $(n+1)s$ levels, then $d^{x-1}s^1$ is not a bad approximation to the configuration or effective valence state of any metal. The filling of the d band increases as one goes to the right in the transition series. But what about the position of the Fermi level? Over the greater part of the transition series it falls, or its magnitude is greater.

What actually happens is shown schematically in Diagram 36, perhaps the single most important diagram of

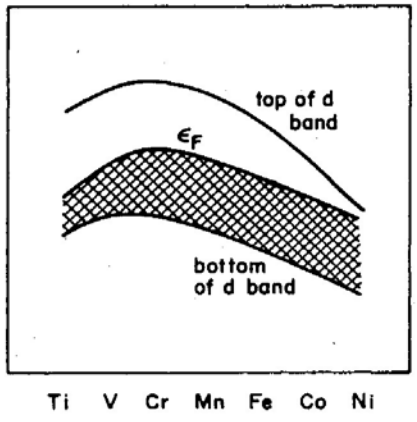

36

metal physics. For a detailed discussion of the band structure the reader is directed to the definitive work of Andersen (1984, 1985). Roughly, what transpires is that the center of gravity of the d band falls as one moves to the right in the transition series. This is a consequence of the ineffective shielding of the nucleus for one d electron by all the other d electrons. The magnitude of the ionization potential of a single d electron increases to the right. The orbitals also become more contracted, hence the less at the right. At the same time, the band filling increases. The position of the band center of gravity and the filling compete; the former wins out. Thus the Fermi level falls at the right side of the transition series. What happens in the middle is a little more complicated (Andersen, 1984, 1985).

Let us see the consequences of this trend for two chemical reactions. One is well studied, the dissociative chemisorption of CO. The other is less well known, but certainly matters, for it must occur in Fischer-Tropsch catalysis. This is the coupling of two alkyl groups on a surface to give an alkane.

In general, early and middle transition metals break up carbon monoxide, late ones just bind it molecularly (Brodén *et al.*, 1976; Engel and Ertl, 1979). *How* the CO is broken up, in detail, is not known experimentally. Obviously, at some point the oxygen end of the molecule must come in contact with the metal atoms, even though the common coordination mode on surfaces, as in molecular complexes, is through the carbon. In the context of pathways of dissociation, the recent discovery of CO lying down on some surfaces (Diagram 37) is intriguing

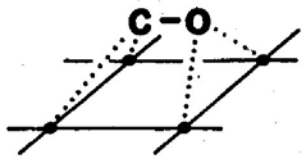

37

(Shinn and Madey, 1984, 1985, 1986; Benndorf, Kruger, and Thieme, 1985; Bardi, Dahlgren and Ross, 1986; see also, for CN^-, Kordesch, Stenzel, and Conrad, 1986; Somers *et al.*, 1987). Perhaps such geometries intervene on the way to splitting the diatomic to chemisorbed atoms. There is a good theoretical model for CO bonding and dissociation (Mehandru, and Anderson, 1986; Mehandru, Anderson, and Ross, 1986).

Parenthetically, the discovery of the situation shown in Diagram 37, and of some other surface species bound in ways no molecular complex shows, should make inorganic and organometallic chemists read the surface literature for reasons other than to find references with which to decorate grant applications. The surface-cluster analogy, of course, is a two-way street. So far, it has been used largely to provide information (or comfort for speculations) for surface studies, drawing on known molecular inorganic examples of binding of small molecules. But now surface structural studies are better, and cases are emerging of entirely novel surface binding modes. Can one design molecular complexes inspired by structures such as Diagram 37?

Returning to the problem of the metal surface influence on the dissociation of CO, we cannot study the reaction path, yet. But we can look at molecular chemisorption, C end bonded, and see if there are any clues. Table III shows one symptom of the bonding on several

TABLE III. Some orbital populations in CO chemisorbed on first transition series surfaces. (From Sung and Hoffmann, 1985.)

	Electron densities in fragment orbitals					
	Ti(0001)	Cr(110)	Fe(110)	Co(0001)	Ni(100)	Ni(111)
5σ	1.73	1.67	1.62	1.60	1.60	1.59
$2\pi^*$	1.61	0.74	0.54	0.43	0.39	0.40

different surfaces, the population of Co 5σ and $2\pi^*$ (Sung and Hoffmann, 1985).

The population of 5σ is almost constant, rising slowly as one moves from the right to the middle. The population of $2\pi^*$, however, rises sharply. Not much is left of the CO bond by the time one gets to Ti. If one were to couple, dynamically, further geometry changes—allowing the CO to stretch, tilt toward the surface, etc.—one would surely get dissociation on the left side of the series.

The reason for these bonding trends is obvious. Diagram 38 superimposes the positions of CO 5σ and $2\pi^*$

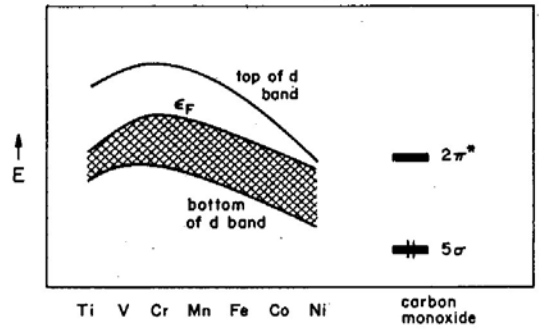

38

levels with the metal *d* band. 5σ will interact more weakly as one moves to the left, but the dramatic effect is on $2\pi^*$. At the right it interacts; that is required for chemisorption. But $2\pi^*$ lies above the *d* band. In the middle and left of the transition series, the Fermi level rises above $2\pi^*$. $2\pi^*$ interacts more, and is occupied to a greater extent. This is the initial indicator of CO disruption. I must say again that there is little novelty about this explanation—it has been obvious to many.

The second case we studied is one specific reaction likely to be important in the reductive oligomerization of carbon monoxide over a heterogeneous catalyst, the Fischer-Tropsch synthesis. The reaction is complicated, and many mechanisms have been suggested. In the one I think likely, the "carbide/methylene" mechanism (R. B. Anderson, 1984), one follows a sequence of breaking up CO and H_2, hydrogenating the carbon to produce methyl, methylene, methyne on the surface, followed by various chain-forming associations of these and terminating reductive eliminations. It is one of those terminal steps I want to discuss here, a prototype dissociation of two adsorbed methyls to give ethane, Diagram 39 (Zheng, Apeloig, and Hoffmann, 1988).

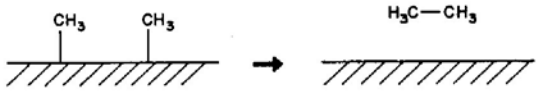

39

Diagram 39 is simple, but it hides a wonderful variety of processes. First, given a surface and a coverage, there is a preferred site that methyls occupy, perhaps an equilibrium between several sites. Second, these methyls must migrate over the surface so as to come near each other. A barrier, call it the "migration energy," may intervene. Third, one methyl's coming into the neighborhood of another may not be enough. It may have to come really close, for instance, on top of a neighboring metal atom. That may cost energy, for one is creating locally a high-coverage situation, one so high that it might normally be inaccessible. One could call this a steric effect, but let us call it a "proximity energy." Fourth, there is the activation energy binding the product molecule to the surface. It is unlikely to be important for ethane (see, however, Wittrig, Szuromi, and Weinberg, 1982; Baetzold, 1983), but might be substantial for other molecules. It is artificial to dissect the reaction in this way; nature does it all at once. But in our poor approach to reality (and here we are thinking in terms of static energy surfaces; we have not even begun to do dynamics, to allow molecules to move on these surfaces), we can think of the components of the barrier impeding coupling: *binding* + *migration* + *proximity* + *coupling* + *desorption* energies.[13]

To be specific, let us choose three dense surfaces: Ti(0001), Cr(110), and CO(0001). The calculations we carried out were for a three-layer slab, and initially a coverage $=\frac{1}{3}$. Three binding sites that were considered were on top or onefold (Diagram 40), bridging or twofold (Diagram 41), capping or threefold (Diagram 42). The preferred site for each metal is the on-top site, Diagram 40.

The total binding energy is greater for Ti than for Cr and greater for Cr than for Co. Diagram 43 is an interaction diagram for CH_3 chemisorption. The CH frontier orbital, a carbon-based directed radical lobe, in-

[13]It should be mentioned that all of the considerations outlined here, as well as those in the original papers on which this work is based, are for ordered overlayers. The true surface dynamics of migration and coupling may proceed in a nonconcerted, nucleated way. The concerted, ordered approach is obviously adapted for computational economy; we try to simulate the true surface reaction by using as low coverage as we can.

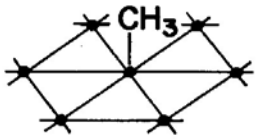

40

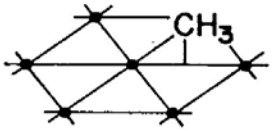

41

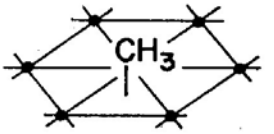

42

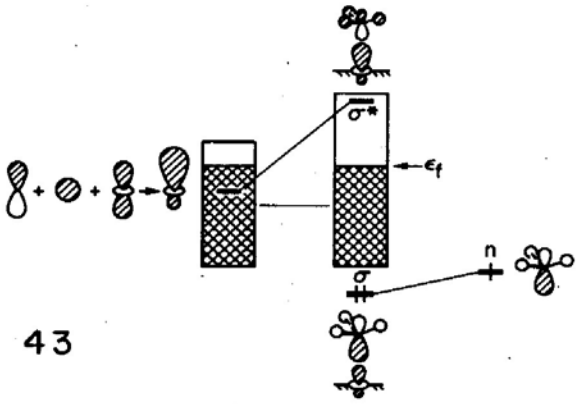

43

teracts with metal s and z^2, much like CO 5σ. Some z^2 states are pushed up above the Fermi level, and this is one component of the bonding. The other is an electron-transfer factor. We started with a neutral surface and a neutral methyl. But the methyl lobe has room for two electrons. Metal electrons readily occupy it. This provides an additional binding energy. And because the Fermi levels increase to the left in the transition series, this ionic component contributes more for Ti than for Co (Zheng, Apeloig, and Hoffmann, 1988).

In a sense, these binding energies of a single ligand are not relevant to the estimation of relative coupling rates of two ligands on different surfaces. But even they show the effect of the Fermi level. A first step in coupling methyls is to consider the migration barriers of isolated groups. This is done in Diagram 44. The relative energy zero in

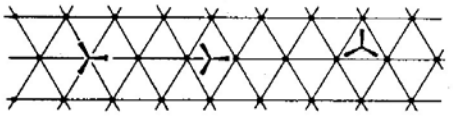

44

Relative E (eV):

Co	0.0	1.1	1.4
Cr	0.0	0.9	0.9
Ti	0.0	0.5	0.1

each case is the most stable on-top geometry.

The implication of Diagram 44 is that for Co the preferred migration itineraries are via bridged transition states, as shown in Diagram 45, but for Ti and Cr surfaces, Diagrams 45 and 46 are competitive. For the reasons behind the magnitudes of the computed barriers, the reader is referred to our full paper (Zheng, Apeloig, and Hoffmann, 1988). Could one design an experiment

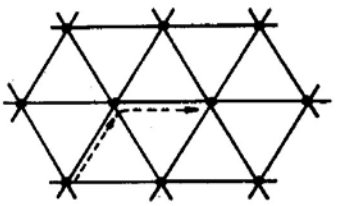

45

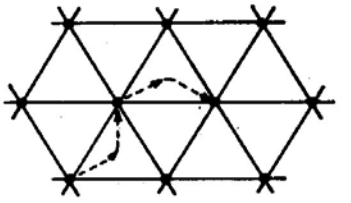

46

to probe these migration alternatives? CH_3 is still an uncommon surface fragment (Tang *et al.*, 1985, 1986).

If we bring two methyl groups to on-top sites on adjacent metals, we see a splitting in the occupied CH_3 states. This is a typical two-orbital four-electron interaction, the way steric effects manifest themselves in one-electron calculations. If we compare the binding energy per methyl group in these proximate structures to the same energy for low-coverage isolated methyls, we get the calculated proximity energies of Diagram 47. The destabilization

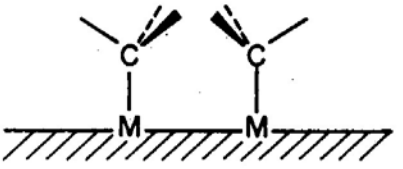

47

Co	0.7 eV
Cr	0.5
Ti	−0.1

increases with d −electron count because some of the d levels occupied carry CH_3 lone pair contributions.

What happens when two CH_3 groups actually couple? The reaction begins with both CH_3 lone pairs nearly

filled, i.e., a representation near CH_3^-. A new C—C σ bond forms, and, as usual, we must consider σ and σ^* combinations, $n_1 \pm n_2$. Both are filled initially, but as the C—C bond forms, the σ^* combination will be pushed up. Eventually, it will dump its electrons into the metal d band.

The actual evolution of the DOS and COOP curves allows one to follow this process in detail. For instance, Fig. 14 shows the contribution of the methyl n orbital, the radical lobe, to the total DOS along a hypothetical coupling reaction coordinate. Note the gradual formation of a two-peaked structure. COOP curves show that the lower peak is C—C bonding, the upper one C—C antibonding. These are the σ and σ^* bonds of the ethane that is being formed.

The total energy of the system increases along the reaction path, as $n_1 - n_2$ becomes more antibonding. At the Fermi level, there is a turning point in the total energy. $\sigma^* = n_1 - n_2$ is vacated. The energy decreases, following $\sigma = n_1 + n_2$. The position of the Fermi level determines the turning point, so the coupling activation energy is greater for Ti than for Cr and greater for Cr than for Co. The reader familiar with reductive eliminations in organometallic chemistry will note essential similarities (Tatsumi *et al.*, 1981; Hoffmann, 1982). We also mention here again the relationship of our argument to the qualitative notions of Mango and Schachtschneider on how coordinated metal atoms affect organic reactions (Mango and Schachtschneider, 1967; Mango, 1978).

The position of the Fermi level and the nature of the states at that level clearly is an important factor in determining binding and reactivity on metal surfaces. This point is not original to this work, but has been clearly discussed in several contributions to the literature (Siegbahn, Blomberg, and Bauschlicher, 1984; Upton, 1984; Harris and Andersson, 1985). The reader's attention is directed to a particularly interesting discussion of how the local DOS at the Fermi level is affected by chemisorption (Feibelman and Hamann, 1985).

XIV. REMARKS

What I have tried to do in this work is to move simultaneously in two directions—to form a link between chemistry and physics by introducing simple band-structure perspectives into chemical thinking about surfaces. And I have tried to interpret these delocalized band structures from a very chemical point of view—frontier orbital considerations based on interaction diagrams.

Ultimately, the treatment of electronic structure in extended systems is no more complicated (nor is it less so) than in discrete molecules. The bridge to local chemical action is through decompositions of the DOS and the crystal orbital overlap population (COOP) curves. These deal with the fundamental questions: Where are the electrons? Where can I find the bonds?

With these tools in hand, one can construct interaction diagrams for surface reactions, as one does for discrete molecules. The warning is that these diagrams are qualitative constructs, within the framework of a one-electron theory. This is not to downgrade them—witness how much they have contributed to our understanding of

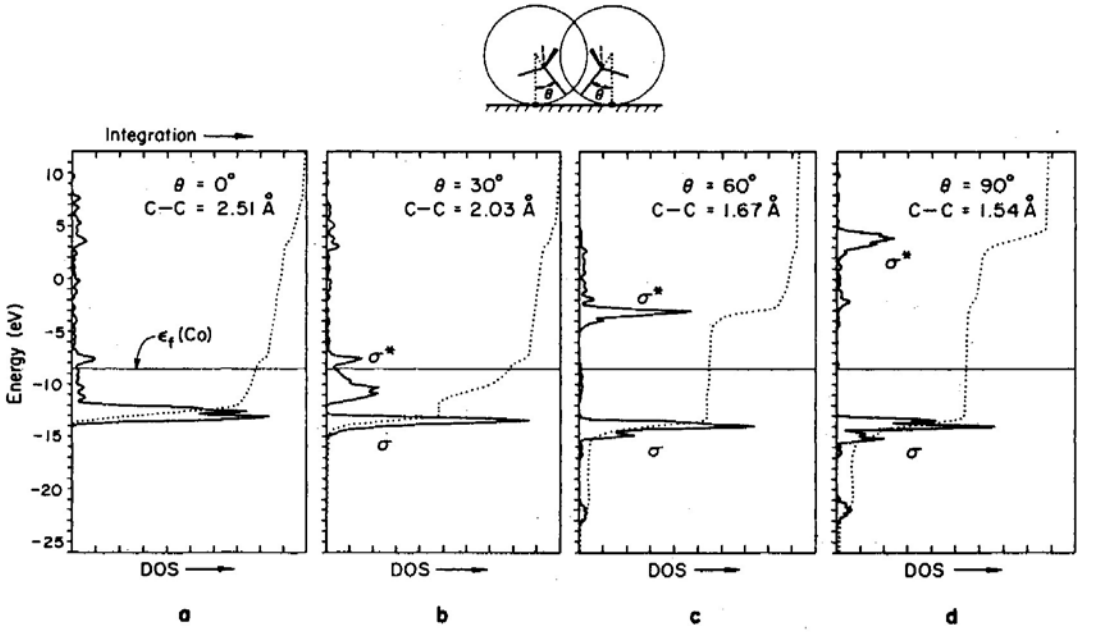

FIG. 14. The evolution of the contribution of methyl lone pairs to the density of states of a chemisorption system [CH_3 on Co(0001)] as the two methyls couple to give ethane. θ is defined at top. Note the development of two peaks corresponding to σ and σ^* of the C—C bond in ethane.

molecular chemistry.

In general, the interactions on a surface resemble those in molecules. The interesting and important differences are two.

(1) There are essential consequences of strong four-electron and zero-electron two-orbital interactions' turning into two-electron ones.

(2) As a corollary, there are shifts of electron density around the Fermi level, which have bonding consequences.

In addition to providing a general picture of bonding of molecules to surfaces, the orbital interaction model, buttressed by detailed DOS and COOP tracing of consequences, provides us with many concepts. We see that effective chemisorption is one point, a compromise, in a continuum that embraces dissociative chemisorption and surface reconstruction. We see how barriers to chemisorption can arise. We see in detail how the Fermi level can influence reactivity. And, not least, we can see the essential electronic similarities and the important differences between bonding in discrete molecules and on surfaces.

ACKNOWLEDGMENTS

The theoretical work of my group in the surface chemistry area was supported initially by the Materials Science Center (MSC) at Cornell University, funded by the Materials Research Division of the National Science Foundation. MSC furnished an interdisciplinary setting, a means of interacting with other researchers in the surface science area, that was very effective in introducing a novice to the important work in the field. I am grateful to Robert E. Hughes, Herbert H. Johnson, and Robert H. Silsbee, the MSC directors, for providing that supporting structure. In the last five years my surface-related research has been generously supported by the Office of Naval Research. That support is in the form of a joint research program with John Wilkins, and led to some joint group meetings that were extremely instructive. Thor Rhodin has been mainly responsible for introducing me to the intellectual riches of surface chemistry and physics, and I am grateful to him and his students for their instruction. The calculations used in our work required much programming and interpretational work. I owe all of this to a remarkable group of co-workers who implemented the band-structure programs with associated graphics. These are Tim Hughbanks, Miklos Kertesz, Myung-Hwan Whangbo, Sunil Wijeyesekera, Charles Wilker, Chong Zheng, and Marja Zonnevylle. Some important ideas were borrowed from Jeremy Burdett. Alfred Anderson was instrumental in getting me started in thinking about applying extended Hückel calculations to surfaces. The band approach, coupled to an interaction diagram and frontier orbital way of thinking, evolved from a study that Jean-Yves Saillard carried out of molecular and surface C-H and H-H activation. We learned a lot together. A subsequent collaboration with Jérôme Silverstre helped to focus many of the ideas in this paper. Important contributions were also made by Yitzhak Apeloig, Susan Jansen, Shen-Shu Sung, Dragan Vučković, Daniel Zeroka, Chong Zheng, and Marja Zonnevylle. I am grateful to Elisabeth Fields and Jane Jorgensen for the great drawings. This manuscript was written while I held the Tage Erlander Professorship of the Swedish Science Research Council. The hospitality of Per Siegbahn at the Institute of Theoretical Physics of the University of Stockholm, and Sten Andersson and Salo Gronowitz of the Chemical Center in Lund, and their staffs, is gratefully acknowledged, as well as the assistance of Jing Li, Jérôme Silvestre, and Marja Zonnevylle in the writing and associated computations.

REFERENCES

Albert, M. R., J. T. Yates, Jr., 1987, *The Surface Scientists Guide to Organometallic Chemistry* (American Chemical Society, Washington).

Albright, T. A., J. K. Burdett, and M.-H. Whangbo, 1985, *Orbital Interactions in Chemistry* (Wiley-Interscience, New York), Chap. 20.

Altman, S. A., 1970, *Band Theory of Metals* (Pergamon, New York).

Andersen, O. K., 1984, in *The Electronic Structure of Complex Systems*, edited by P. Phariseau and W. M. Temmerman (Plenum, New York), p. 11.

Andersen, O. K., 1985, in *Highlights of Condensed Matter Physics*, edited by F. Bassani, F. Fumi, and M. P. Tossi (North-Holland, New York), p. 59.

Anderson, A. B., 1977, J. Am. Chem. Soc. **99**, 696.

Anderson, A. B., and S. P. Mehandru, 1984, Surf. Sci. **136**, 398.

Anderson, R. B., 1984, *The Fischer-Tropsch Synthesis* (Academic, New York).

Andreoni, W., and C. M. Varma, 1981, Phys. Rev. B **23**, 437.

Andzelm J., and D. R. Salahub, 1986, Int. J. Quantum. Chem. **29**, 1091.

Ashcroft, N. W., and N. D. Mermin, 1976, *Solid State Physics* (Holt, Rinehart and Winston, New York).

Avouris, Ph., P. S. Bagas, and C. J. Nelin, 1986, J. Electron. Spectrosc. Relat. Phenom. **38**, 269.

Baetzold, R. C., 1983, J. Am. Chem. Soc. **105**, 4271.

Baetzold, R. C., 1988, in *Catalysis*, edited by J. Moffatt, in press.

Banholzer, W. F., Y. O. Park, K. M. Mak, and R. I. Masel, 1983, Surf. Sci. **128**, 176.

Bardi, V., D. Dahlgren, and N. Ross, 1986, J. Catal. **100**, 196.

Benndorf, C., B. Kruger, and F. Thieme, 1985, Surf. Sci. **163**, L675.

Bigot, B., and C. Minot, 1984, J. Am. Chem. Soc. **106**, 6601.

Blyholder, G., 1964, J. Phys. Chem. **68**, 2772.

Brodén, G. T. N. Rhodin, C. Brucker, H. Benbow, and Z. Hurych, 1976, Surf. Sci. **59**, 593.

Burdett, J. K., 1984, Prog. Solid State Chem. **15**, 173.

Chan, C.-M., and M. A. Van Hove, 1986, Surf. Sci. **171**, 226.

Chatt, J., and L. A. Duncanson, 1953, J. Chem. Soc. 2939.

Christmann, K., 1987, Z. Phys. Chem. **154**, 145.

Cohen, M. L., 1984, Annu. Rev. Phys. Chem. **34**, 537.

Cox, P. A., 1987, *The Electronic Structure and Chemistry of Solids* (Oxford University Press, Oxford).

Daum, W., S. Lehwald, and H. Ibach, 1986, Surf. Sci. **178**, 528.

Dewar, M. J. S., 1951, Bull. Soc. Chim. Fr. **18**, C71.

Dewar, M. J. S., 1969, *The Molecular Orbital Theory of Organic Chemistry* (McGraw-Hill, New York).

Elian, M., and R. Hoffmann, 1975, Org. Chem. **14**, 1058.
Engel, T., and G. Ertl, 1979, Adv. Catal. **28**, 1.
Feibelman, P. J., and D. R. Hamann, 1985, Surf. Sci. **149**, 48.
Fujimoto, H., 1987a, Accts. Chem. Res. **20**, 448.
Fujimoto, H., 1987b, J. Phys. Chem. **91**, 3555.
Fujimoto, H., M. Kawamura, T. Ichiishi, and K. Fukui, J. Mol. Str. Theochem., in press.
Fukui, K., 1982, Science **218**, 747.
Gadzuk, J. W., 1974, Surf. Sci. **43**, 44.
Garfunkel, E. L., and X. Feng, 1986, Surf. Sci. **176**, 445.
Garfunkel, E. L., C. Minot, A. Gavezzotti, and M. Simonetta, 1986, Surf. Sci. **167**, 177.
Gavezzotti, A., and M. Simonetta, 1980, Adv. Quantum Chem. **12**, 103.
Grimley, T. B., 1971, J. Vac. Sci. Technol. **8**, 31.
Grimley, T. B., 1972, in *Adsorption-Desorption Phenomena,* edited by F. Ricca (Academic, London/New York), p. 215.
Hamza, A. V., H.-P. Steinruck, and R. J. Madix, 1987, J. Chem. Phys. **86**, 6506.
Harris, J., and S. Anderson, 1985, Phys. Rev. Lett. **55**, 1583.
Harrison, W. A., 1980a, *Electronic Structure and Properties of Solids* (Freeman, San Francisco).
Harrison, W. A., 1980b, *Solid State Theory* (Dover, New York).
Hjelmberg, H., B. I. Lundqvist, and J. K. Nørskov, 1979, Phys. Scr. **20**, 192.
Hoffmann, R., 1963, J. Chem. Phys. **39**, 1397.
Hoffmann, R., 1982, in IUPAC, *Frontiers in Chemistry,* edited by K. J. Laidler (Pergamon, Oxford), p. 247.
Hoffmann, R., 1987, Angew. Chem. **99**, 871 [Angew. Chem. Int. Ed. Engl. **26**, 846 (1987)].
Hoffmann R., and W. N. Lipscomb, 1962, J. Chem. Phys. **36**, 2179.
Holloway, S., B. I. Lundqvist, and J. K. Nørskov, 1984, in *Proceedings of the 8th International Congress on Catalysis* (Springer, Berlin), Vol. 4, p. 85.
Hughbanks, T., and R. Hoffmann, 1983, J. Am. Chem. Soc. **105**, 3528.
Inglesfield, J. E., 1985, Prog. Surf. Sci. **20**, 105.
Jorgensen, W. L., and L. Salem, 1973, *The Organic Chemist's Book of Orbitals* (Academic, New York).
Kang, D. B., and A. B. Anderson, 1985, Surf. Sci. **155**, 639.
Kang, D. B., and A. B. Anderson, 1986, Surf. Sci. **165**, 221.
Kasowski, R. V., T. Rhodin, and M.-H. Tsai, 1986, Appl. Phys. A **41**, 61.
Kertesz, M., and R. Hoffmann, 1984, J. Am. Chem. Soc. **106**, 3453.
Kesmodel, L. L., L. H. Dubois, and G. A. Somorjai, 1979, J. Chem. Phys. **70**, 2180.
King, D. A., 1983, Phys. Scr. **4**, 34.
Kleinle, G., V. Penka, R. J. Behm, G. Ertl, and W. Moritz, 1987, Phys. Rev. Lett. **58**, 148.
Kohn, W., and L. J. Sham, 1965, Phys. Rev. **140**, 1133A.
Kordesch, M. E. , W. Stenzel, and H. Conrad, 1986, J. Electron Spectrosc. Relat. Phenom. **38**, 89.
Koutecký J., and P. Fantucci, 1986, Chem. Rev. **86**, 539.
LaFemina, J. P., and J. P. Lowe, 1986, J. Am. Chem. Soc. **108**, 2527.
Lang, N. D., 1983, in *Theory of the Inhomogeneous Electron Gas,* edited by S. Lundqvist and N. H. March (Plenum, New York), p. 309.
Lang, N. D., and J. K. Nørskov, 1983, Phys. Rev. B **27**, 4612.
Lang, N. D., and A. R. Williams, 1976, Phys. Rev. Lett. **37**, 212.
Lang, N. D., and A. R. Williams, 1978, Phys. Rev. B **18**, 616.
Lo, T.-C., and G. Ehrlich, 1987, Surf. Sci. **179**, L19.
Lundqvist, B. I., 1983, Vacuum **33**, 639.
Lundqvist, B. I., 1984, in *Many-Body Phenomena Surfaces,* edited by D. C. Langreth and H. Suhl (Academic, New York), p. 93.
Lundqvist, B. I., 1986, Chem. Scr. **26**, 423.
Lundqvist, B. I., J. K. Nørskov, and H. Hjelmberg, 1981, Surf. Sci. **80**, 441.
Mango, F. D., 1978, Coord. Chem. Rev. **15**, 109.
Mango, F. D., and J. H. Schachtschneider, 1967, J. Am. Chem. Soc. **89**, 2848.
Masel, R. I., 1988, unpublished.
Mehandru, S. P., and A. B. Anderson, 1986, Surf. Sci. **169**, L281.
Mehandru, S. P., and A. B. Anderson, and P. N. Ross, 1986, J. Catal. **100**, 210.
Messmer, R. P., 1977, in *Semiempirical Methods of Electronic Structure Calculation, Part B: Applications,* edited by G. A. Segal (Plenum, New York), p. 215.
Messmer, R. P., and A. J. Bennett, 1972, Phys. Rev. B **6**, 633.
Mingos, D. M. P., 1972, Nature (Phys. Sci.) **236**, 99.
Minot, C., B. Bigot, and M. Hariti, 1986, Nouv. J. Chim. **10**, 461.
Minot, C., M. A. Van Hove, and G. A. Somorjai, 1983, Surf. Sci. **127**, 441.
Muetterties, E. L., 1978, Angew. Chem. Int. Ed. Engl. **17**, 545.
Muetterties, E. L., 1982, Chem. Soc. Rev. **11**, 283.
Muetterties, E. L., and T. N. Rhodin, 1979, Chem. Rev. **79**, 91.
Mulliken, R. S., 1955, J. Chem. Phys. **23**, 1833; **23**, 2343.
Nørskov, J. K., S. Holloway, and N. D. Lang, 1984, Surf. Sci., **137**, 65.
Nørskov, J. K., A. Houmøller, P. K. Johansson, and B. I. Lundqvist, 1981, Phys. Rev. Lett. **46**, 257.
Nørskov, J. K., and N. D. Lang, 1980, Phys. Rev. B **21**, 2136.
Raatz, F., and D. R. Salahub, 1984, Surf. Sci. **146**, L609.
Rhodin T. N., and G. Ertl, 1979, Eds., *The Nature of the Surface Chemical Bond* (North-Holland, Amsterdam).
Saillard, J.-Y., and R. Hoffmann, 1984, J. Am. Chem. Soc. **106**, 2006.
Salahub, D. R., and F. Raatz, 1984, Int. J. Quantum. Chem. Symp. No. 18, 173.
Salem, L., 1985, J. Phys. Chem. **89**, 5576.
Salem, L., and R. Elliott, 1983, J. Mol. Struct. **93**, 75.
Salem, L., and R. Lefebvre, 1985, Chem. Phys. Lett. **122**, 342.
Salem, L., and C. Leforestier, 1979, Surf. Sci. **82**, 390.
Shinn, N. D., and T. E. Madey, 1984, Phys. Rev. Lett. **53**, 2481.
Shinn, N. D., and T. E. Madey, 1985, J. Chem. Phys. **83**, 5928.
Shinn, N. D., and T. E. Madey, 1986, Phys. Rev. B **33**, 1464.
Shustorovich, E. M., 1985, Surf. Sci. **150**, L115.
Shustorovich, E. M., 1986, Surf. Sci. **6**, 1.
Shustorovich, E. M., 1987, J. Phys. Chem. **87**, 14.
Shustorovich, E. M., and R. C. Baetzold, 1985, Science **227**, 876.
Siegbahn, P. E. M., 1988, unpublished.
Siegbahn, P. E. M., M. R. A. Blomberg, and C. W. Bauschlicher, Jr., 1984, J. Chem. Phys. **81**, 2103.
Silvestre, J., and R. Hoffmann, 1985, Langmuir 1, 621.
Somers, J., M. E. Kordesch, Th. Lindner, H. Conrad, A. M. Bradshaw, and G. P. Williams, 1987, Surf. Sci. **188**, L693.
Somorjai, G. A., 1981, *Chemistry in Two Dimensions* (Cornell University Press, Ithaca).
Steinruck, H.-P., A. V. Hamza, and R. J. Madix, 1986, Surf. Sci. **173**, L571.
Sung, S., and R. Hoffmann, 1985, J. Am. Chem. Soc. **107**, 578.
Tang, S. L., J. D. Beckerle, M. B. Lee, and S. T. Ceyer, 1986, J.

Chem. Phys. **84**, 6488.
Tang, S. L., M. B. Lee, J. D. Beckerle, M. A. Hines, and S. T. Ceyer, 1985, J. Chem. Phys. **82**, 2826.
Tatsumi, K., R. Hoffmann, A. Yamamoto, and J. K. Stille, 1981, Bull. Chem. Soc. Jpn. **54**, 1857, and references therein.
Thorpe, B. J., 1972, Surf. Sci. **33**, 306.
Upton, T. H., 1984, J. Am. Chem. Soc. **106**, 1561.
von Doorn, W., and J. Koutecký, 1977, Int. J. Quantum Chem. **12**, (Suppl. 2), 13.
Van Hove, M. A., R. J. Koestner, P. C. Stair, J. P. Bibérian, L. L. Kesmodel, I. Bartos, and G. A. Somorjai, 1981, Surf. Sci. **103**, 189, 218.
van Santen, R. A., 1984, in *Proceedings of the 8th International Congress on Catalysis* (Springer, Berlin), Vol. IV, p. 97.
van Santen, R. A., 1986, Faraday Symp. Chem. Soc. **21**.
Varma, C. M., and A. J. Wilson, 1980, Phys. Rev. B **22**, 3795.
Wade, K., 1971a, Chem. Commun. 792.
Wade, K., 1971b, *Electron Deficient Compounds* (Nelson, London).
Wade, K., 1972, Inorg. Nucl. Chem. Lett. **8**, 559.
Whangbo, M.-H., 1986, in *Crystal Chemistry and Properties of Materials with Quasi One-Dimensional Structures,* edited J. Rouxel (Reidel, Dordrecht), p. 27.
Wijeyesekera, S. S., and R. Hoffmann, 1984, Organometallics **3**, 949.
Wilson, A. J., and C. M. Varma, 1980, Phys. Rev. B **22**, 3805.
Wittrig, T. S., P. D. Szuromi, and W. H. Weinberg, 1982, J. Chem. Phys. **76**, 3305.
Zheng, C., Y. Apeloig, and R. Hoffmann, 1988, J. Am. Chem. Soc., **110**, 749.